

ANALYSIS OF FLUIDITY OF METALS

by

John E. Niesse

B.S., United States Naval Academy
(1950)

S. M., Massachusetts Institute of Technology
(1956)

SUBMITTED IN PARTIAL FULFILLMENT
OF THE REQUIREMENTS FOR THE
DEGREE OF
DOCTOR OF SCIENCE
at the
MASSACHUSETTS INSTITUTE OF TECHNOLOGY
September, 1958

Signature of Author _____
Department of Metallurgy, September 1958

Certified by _____ Thesis Supervisor

Thesis Supervisor

Accepted by _____
Chairman, Departmental Committee
on Graduate Students

ANALYSIS OF FLUIDITY OF METALS

by

John E. Niesse

Submitted to the Department of Metallurgy on 5 September 1958
in partial fulfillment of the requirements for the degree of Doctor of
Science.

ABSTRACT

Fluidity, in the foundry sense, was investigated in an attempt to express it quantitatively. Experiments were made on the tin-lead binary system to verify the analytical findings and to define the nature and extent of various mechanisms of solidification.

By use of heat flow and fluid flow equations, the fluidity of a pure metal at its melting point was expressed in the form of a differential equation. The effect of superheat was indicated, but this equation was more difficult to solve. The shape of the solid-liquid interface was found to be parabolic. The effect of superheat for pure metals and alloys depended on the fluid life of the metal stream: with a short fluid life the effect was limited to the length for initial removal of superheat.

Experimentally three distinct areas of fluidity were found in the tin-rich side of the tin-lead binary system. The highest fluidity was found at pure - or nearly pure - tin where "plane front" freezing is typical. At higher lead content the fluidity dropped rapidly. Above about 1% lead the fluidity was low and practically constant. In the last area the mechanism of freezing was shown to be caused by dendrites choking the flow off very rapidly at the mold entrance if the metal was poured at the liquidus temperature.

Thesis Supervisor: Merton C. Flemings, Jr., Assistant Professor
of Metallurgy

TABLE OF CONTENTS

	<u>Page</u>
Abstract	ii
Table of Contents	iii
List of Figures	v
List of Tables	vii
List of Symbols	viii
Acknowledgments	x
I Introduction	1
II Literature Survey	3
III Plan of Research	6
IV Analytical Approach	8
Heat Flow Analysis	8
Fluid Flow Analysis	10
Case of No Freezing	10
Case of No Superheat	11
Case with Superheat - Pure Metal	12
Case with Superheat - Alloys	13
V Experimental Approach	14
Apparatus	14
Procedure	15
Results	16
Discussion	18
VI Conclusions	22
Suggestions for Future Work	24
Bibliography	36

Appendices

A	Quantitative Analyses in the Literature	40
B	Determining Energy Lost from Solid Metal Before Flow Ceases for Pure Metals	50
C	Evaluation of Friction Factor	53
D	Heat Flow in Cylindrical Channels	57
E	Factors Affecting Velocity	60
F	Evaluating Shapes of Solid-Liquid Interface for Pure Tin	62
G	Calculation of Minimum Increase of Fluidity Due to Superheat	68
H	Limits of Validity of Equation (1)	70
I	Physical Properties of Pyrex Glass	73
J	Fluidity and Fluid Life Data	77
	Biographical Note	86

LIST OF FIGURES

<u>Figure</u>	<u>Title</u>	<u>Page</u>
1	Curves of Fluidity Versus Time Comparing Analytical (Equation 6) to Experimental	25
2	Schematic Sketch of Vacuum Fluidity Apparatus ...	26
3	Comparison Fluidity of Pure Tin with Data from Ragone	27
4	Fluidity and Fluid Life as a Function of Log Composition	28
5	Fluidity, Fluid Life, and Slope of Fluidity-Temperature Curves as a Function of Composition at Liquidus Temperature	29
6	Fluidity and Initial Velocity as Functions of the Square Root of Metal Head	30
7	Fluidity as a Function of Freezing Time for Various Metal Heads and Alloys at Liquidus Temperatures	31
8	Distance as a Function of Time for Tin - 5.1% Lead Alloys	32
9	Distance Versus Time for Tin-Lead Alloys at 240°C	33
10	Schematic Curves Showing the Increased Influence of Zone II with Increased Fluidity	34
11	Total Energy Removed from Metal Prior to Cessation of Flow for 5.1% Lead Alloys	36
A1	Klyachko and Kunin Graph of Relative Fluidity	48
A2	Ruff's Graph of Stationary Wall Thickness as a Function of Metal Velocity at the Wall	49
B1	Schematic Cross Section of Fluidity Stream at the Time Flow Ceases	51
B2	Energy from Solid Metal as a Function of Freezing Time and Tube Radius	52

<u>Figure</u>	<u>Title</u>	<u>Page</u>
C1	Reynolds Number for Fluidity Tests from Equation (C1).....	55
C2	Friction Factor Versus Reynolds Number in Long, Straight Ducts (after Moody).....	56
D1	Schematic Temperature Distribution in Metal and Mold	59
F1	Solid-Liquid Interfaces for $V_i = 180$ cm/sec.....	65
F2	Solid-Liquid Interfaces for $V_i = 100$ cm/sec.....	66
F3	Stream Velocity as a Function of Time, θ , and Length, L_e	67
H1	Heat Absorption Ability of Infinite and Finite Plates Compared	72
I1	Heat Content and Thermal Conductivity of Pyrex Glass as Functions of Temperature.....	75
I2	Freezing Time for Tin as a Function of Distance Between Pyrex Plates	76
J1	Fluidity at Ten Inches Metal Head, Small Tubes	78
J2	Fluidity of Pure Tin, Small Tubes	79
J3	Fluidity of 5.1% Lead Alloys - Small Tubes.....	80
J4	Fluidity of 5.1% Lead Alloys - Large Tubes	81
J5	Fluid Life at Ten Inches Metal Head.....	82
J6	Fluid Life of Pure Tin, Small Tubes	83
J7	Fluidity of Tin-Lead Alloys as a Function of Fluid Life	84
J8	Fluid Life of 5.1% Lead Alloys - Large Tubes	85

LIST OF TABLES

<u>Table</u>	<u>Title</u>	<u>Page</u>
I	Start of Solution of Equation (2) Using Iterative Process	64
II	Calculation of Decrease in Temperature for Superheated Metal	69

LIST OF SYMBOLS

A	$2R/\sqrt{\pi\alpha'} \quad \text{sec}^{1/2}$
B	$(1 + 2Rh/k')$
c	specific heat of molten metal, cal/gm°C
c'	specific heat of mold material, cal/gm°C
D	diameter of mold channel, cm
f	friction factor
g	acceleration due to gravity, cm/sec ²
h	heat-transfer coefficient at metal-mold interface, cal/°C cm ² sec
H	heat of fusion of metal, cal/gm
k	thermal conductivity of metal, cal/sec cm ² °C/cm
k'	thermal conductivity of mold
L	length along metal stream
L _e	length to end of metal stream
L _f	"Fluidity" or final length of metal stream
N _{Re}	Reynolds number, $\frac{VD\rho}{\mu}$
q	heat flow rate, cal/sec
Q	total heat entering mold material per unit length in time θ_h , cal/cm sec
r	radius of liquid metal in mold, cm
R	radius of mold channel, cm
t	thickness of slabs, cm
T	temperature of liquid metal, °C
T _i	initial or pouring temperature, °C

T_m	melting temperature or liquidus temperature, °C
T_o	temperature at zero fluidity (extrapolated), °C
T_r	room temperature (25°C) or initial mold temperature, °C
T_{sc}	temperature of mold at metal-mold interface
T'	$\frac{T_i - T_r}{T_m - T_r}$ = relative superheat
V	average metal velocity at any cross section, cm/sec
V_e	instantaneous velocity of end of metal stream, cm/sec
V_i	initial velocity of metal stream, $\sqrt{\frac{2gZ}{1 + \phi_{ent}}}$,
Z	height of metal head, cm
α	thermal diffusivity of metal, cm ² /sec
α'	thermal diffusivity of mold, cm ² /sec
θ	time after metal starts to flow, sec
θ_h	time after metal-mold contact, sec
θ_f	final freezing time, sec
\mathcal{K}	$\sqrt{\frac{\rho'c'k'}{\pi}}$
μ	viscosity, poise
ρ	metal density, gm/cm ³
ρ'	mold density, gm/cm ³
ϕ_{ent}	entrance loss coefficient

ACKNOWLEDGEMENTS

The author wishes to acknowledge the guidance and understanding of Professors H. F. Taylor, M. C. Flemings, and C. M. Adams who saw this work through from its inception and whose counsel during many discussions was invaluable.

The aid from Crane Company in the form of a fellowship grant was a generous financial help which made this work possible and is gratefully acknowledged.

The author wishes to thank all those of the Foundry Staff for their help and patience.

I INTRODUCTION

The "fluidity" of molten metal is defined as the distance it will flow in a channel of specified size and shape before freezing stops the flow; fluidity is measured in units of length and depends on the physical properties of metal and mold materials as well as the conditions of the test.

There is little dispute over the fact that metal stops flowing due to the effects of freezing. Certainly a pure metal which freezes with a smooth and definite solid-liquid interface (commonly known as "plane front" freezing), ceases to flow because of the growth of solid from the mold wall into the flowing liquid. However, with alloys which freeze under other mechanisms (not well understood), the exact nature of the solid which stops the flow is not well known. In fact there is much discussion over this question of the nature of the solid.

Until one has a basic understanding of the formation of solid in a test piece used to measure the fluidity of alloys, no fundamental analysis of the characteristics of fluid flow is possible. In general the following points are known about alloy solidification: 1) the typical shape of the solid is dendritic characterized by irregular needle-like or pine-tree-like shapes, 2) a large freezing interval, or distance between the liquidus and solidus temperatures, increases the tendency to form dendrites and/or accentuates the sharpness of the needle-like shape, and 3) a high temperature gradient decreases the extent of dendrite formation and may change the solidification to the "plane front" type.

One of the objectives of this thesis is to increase the understanding of the process of alloy solidification under fluidity test conditions. Obviously thermal and other conditions that control freezing are of great importance as well as the mode of freezing itself.

II LITERATURE SURVEY

The recorded study of fluidity of metals started many years ago (1898) and has had numerous contributors. All have used a mold channel of small cross section and measured fluidity as the length or amount of metal the mold contained after pouring.

Bibliographies

Excellent bibliographies on the subject of fluidity have been compiled by Briggs⁵, Ragone et al.⁴², Clark⁶ and Krynitsky²³.

Types of Fluidity Testers

The first tester used was a sand wedge⁵³. The early part of this century saw horizontal straight channels of round cross section used by many investigators. The mold materials have been sand⁴⁵, metal^{40, 33}, and glass⁴³. A new "star-type" tester has been recently developed consisting of radially oriented flat, horizontal channels in a sand mold²⁰. U-shaped testers have been used by Evans¹² and Nekhendzi and Samarin¹⁸. The most popular and most developed tester in this country by far is the spiral tester. The history of this tester is excellently described by Krynitsky²³ and Clark⁶. There have been many modifications to the spiral tester to increase reproducibility. The accepted standards for iron and steel are those designs by Saeger and Krynitsky⁴⁷ and Taylor et al.⁴⁹. The cross-sectional shape of the mold channel has also been changed, the most radical being a change from a bulk shape to a flat shape to emphasize surface effects in aluminum alloys^{11, 30}. The

vacuum fluidity tester⁴³ used tubes as mold channels, and instead of pouring metal, it was pulled into the mold by a partial vacuum.

Variables of Testing

In general these variables are gating method; control of casting head; mold properties such as surface characteristics, physical properties, permeability of sand, etc.; rate of pouring; and superheat. These are adequately described and discussed by many authors^{5, 20, 23, 6, 21, 45}. In general the problems of testing control and measurement have been solved with reasonable success for practical purposes and, to a lesser extent, for research purposes. Measurement of metal velocity has been accomplished by three different means: photographic motion pictures^{25, 45, 40}, closing of electrical circuits^{25, 7}, and by measuring the length the stream travels horizontally for a given vertical drop⁴⁵.

Metal Variables

Probably most of the disagreement in the study of fluidity comes in this area. The factors of importance have been reviewed adequately by Portevin and Bastien³⁷, Ragone et al.⁴², Desch⁸, and Kondic¹⁹. In general the most reliable conclusions are that superheat is of prime importance in the fluidity of alloys^{6, 21, 54, 35, 44, 42} and that fluidity varies inversely as the freezing interval (liquidus to solidus temperatures)^{36, 43, 21, 3, 33}. Other variables are generally of minor importance.

Surface tension is of minor importance^{24, 19, 44} in general; however, aluminum may be an exception as Klyachko and Kunin¹⁸ claim to have observed an increase in fluid velocity of almost 100% due to surface tension of aluminum³⁰.

Surface films may be important in fluidity because they may increase the effective surface tension, if solid they may cause mechanical interference to flow, or they may change heat-transfer coefficients at the metal-mold interface^{19, 39, 8}.

Viscosity is now considered to be of minor importance in fluidity⁴².

Solidification characteristics certainly have an important effect on fluidity. These characteristics are the result of freezing interval. In short, round or convex faced crystals yield a much higher fluidity than dendritic crystals^{37, 27} due to lower frictional energies encountered with round crystals. Eutectics may solidify in round crystals and alloys with a wide freezing interval solidify dendritically. The applicability of these theories of crystal shape to freezing of metals in fluidity tests has yet to be proven.

Fluidity of Iron and Steel

The fluidity of iron and steel has received much attention. As in other fields, iron and steel seems to have its own particular problems in addition to its fluidity variables. In order not to complicate the study of fluidity itself, only a bibliography of iron and steel will be given here. Those who have contributed most to this field are refs.^{45, 15, 3, 2, 52, 48, 55, 22, 4, 51, 12, 26, 34, and 46}.

Quantitative Analyses of Fluidity

Due to the fact that a recent review of analyses has not been found in the literature, and also because this thesis is, in part, a quantitative analysis, a detailed review of the literature in this area has been prepared and is presented in Appendix A.

III PLAN OF RESEARCH

This research is to be divided into two general headings: 1) the analytical approach and (2) experimental. These sections are not intended to be isolated, but a mutual interchange between the two exists such that the conclusions of the one section aid or support the other section. Briefly the objectives of each section are:

- I. Analytical Approach
 - A. Derive a valid general equation governing heat flow in fluidity channels of circular cross section.
 - B. Using the laws of fluid flow and the results of the heat flow analyses derive a relation for fluidity of a pure metal at its melting point, and at any degree of superheat.
 - C. Attempt to find a relation for the fluidity of alloys with superheat.
- II. Experimental Approach
 - A. Build a suitable apparatus for measuring fluidity as well as measuring velocity of the stream.
 - B. Measure fluidity and length versus time of various alloys of a typical eutectic system and attempt to identify composition limits for various fluidity mechanisms.

- C. Determine effect of pressure, size of channels, and superheat on fluidity.
- D. Attempt to determine the mechanism governing the solidification of mushy alloys in fluidity tests.

IV ANALYTICAL APPROACH

In addition to physical properties such as heat of fusion, viscosity, density, etc., the factors of importance in fluidity may be classed as 1) those which affect the heat flow through metal, mold, and mold wall, 2) those which affect the fluid flow, and 3) the solidification characteristics of the metal. Fluid flow and heat flow have been investigated in connection with other fields and these results have proven applicable to metal flow^{42, 44}. Most studies have over-simplified these relations especially where heat flow is concerned. The solidification characteristics of alloys in fluidity tests are still under debate and therefore any basic analysis of fluidity of alloys is necessarily debatable. The experimental section of this thesis will throw some light on the mechanism governing the solidification of alloys in fluidity tests.

Heat Flow Analysis

The energy or heat which enters the mold may arise from super-heated liquid metal, heat of fusion, or cooling of the solid metal below the freezing temperature. Appendix B shows that the energy involved in cooling solid metal before flow ceases is negligible.

The heat flow path for metal in a fluidity mold embraces resistances in 1) the liquid metal, 2) the liquid metal boundary layer, 3) the solid (or stationary liquid) metal, if any, 4) the mold wall boundary, and 5) the mold. Where turbulent metal flow is encountered, as in practically all fluidity tests (see Appendix C and ref. 44), the radial heat flow resistance in the liquid metal is negligible due to convection. Turbulence,

relatively high coefficient of heat conductivity of metals, and the fact that most of the heat originates from heat of fusion all tend to make boundary layer resistance negligible compared to other factors. Appendix B shows that, prior to cessation of flow, heat flow resistance in the solid metal is negligible. Thus a good approximation of heat flow assumes heat flow resistances at the metal-mold interface and in the mold.

Assuming a round mold channel and a mold material with low heat conductivity (such as sand or glass), equation (1) for the removal of heat as a function of time can be derived. (See Appendix D for details.)

$$Q = \frac{2Rh\pi(T-T_r)}{B} \left\{ \theta_h + 2A\left(1-\frac{1}{B}\right)\sqrt{\theta_h} - \frac{2A^2}{B}\left(1-\frac{1}{B}\right)\ln\left(1+\frac{B}{A}\sqrt{\theta_h}\right) \right\} \quad (1)$$

where Q = energy removed in cal/sec/cm of length

$$A = 2R / \sqrt{\pi\alpha'} \quad \text{sec}^{1/2}$$

$$B = (1 + 2Rh/k')$$

Equation (1) defines the heat removed as a function of time. The physical properties required are those of the mold material (ρ' , c' , and k') and the interface heat transfer coefficient, h .

The mold physical properties do vary with temperature, especially the heat content and the thermal conductivity. In Appendix I it is shown that average effective values of these properties are at a temperature closer to the metal temperature than to the original mold temperature. This fact was shown for tin freezing between pyrex glass plates, and the results are applicable to this work. The glass properties for 200°C are the effective values for the freezing of tin.

The value of h must be found empirically, similar to the method of Ragone⁴², by letting Q equal the heat of fusion for unit length of pure tin; θ then equals the final freezing time, θ_f . The value of θ_f must be found

experimentally. When R was 0.193 cm, θ_f for pure tin at the melting temperature was 1.45 sec. These values used in equation (1) give h equal to 0.18 cal/cm², °C, sec, a reasonable value which is used throughout this work.

Fluid Flow Analysis

The fluid flow analysis stems from an energy balance using Bernoulli's equation similar to that done by Ragone⁴². Acceleration effects are assumed negligible and metal head is assumed constant. If "plane front" freezing is assumed - characteristic of pure metals - the result is equation (2) (see Appendix E):

$$\frac{dL_e}{d\theta} = V_e = \frac{V_i}{\sqrt{1 + \frac{fR^4}{2(1+\phi_{ent})} \int_0^{L_e} \frac{dL}{r^5}}} \quad (2)$$

The values of ϕ_{ent} and f were evaluated empirically. From motion pictures of the metal stream and equation (E5), $V_i = \sqrt{\frac{2gZ}{1+\phi_{ent}}}$, ϕ_{ent} was found to be about 0.95, which is a reasonable value considering that the entrance loss (usually taken as 0.8) and the energy loss in the bend in the tubes are lumped in ϕ_{ent} . The evaluation of f required the solution of equation (2) and then comparison with an experimental fluidity test (see Figure 1). A value of f equal to about 0.05 was found to satisfy the comparison.

Case of no Freezing

Equation (2) is a general form. If no freezing occurs, as is the case for initial parts of fluidity tests with superheated metal and alloys, r is constant and equal to R , the channel radius. Then equation (2) becomes:

$$\frac{dL_e}{d\theta} = V_e = \frac{V_i}{\sqrt{1 + \frac{f}{2(1+\phi_{ent})R} L_e}} \quad (3)$$

which can be integrated (see Appendix E):

$$L_e = \frac{2(1 + \phi_{ent})R}{f} \left[\left(\frac{3}{4} \frac{f V_i \theta}{(1 + \phi_{ent})R} + 1 \right)^{2/3} - 1 \right] \quad (4)$$

Case of no Superheat

A pure metal freezes in a characteristic manner, that is the liquid-solid interface is an isotherm - the freezing temperature. This mode of freezing usually results in smooth interfaces. Hence the name "plane front". Such a mechanism yields a solid, smooth cylinder of metal in a cylindrical fluidity mold. Thus r , the radius of the liquid metal channel, is a definite and determinable quantity. If r can be expressed in terms of L , then the integral in equation (2) may be solved.

In Appendix F, equations (1) and (2) were used in a numerical solution. Curve fitting showed that r and L were related parabolically as expressed in equation (5):

$$r = R - K\sqrt{L_e - L} \quad (5)$$

where K is a function of V_e . The function may vary as the conditions of the fluidity test change. As explained in Appendix F, equation (5) does not apply as the metal velocity approaches zero, that is, toward the end of the fluidity run. Therefore numerical solutions based on equation (5) are not valid for velocities lower than about 15 cm/sec. However, at this velocity the metal has run about 95% of its total distance.

Substituting (5) in (2) and integrating yields:

$$\frac{dL_e}{d\theta} = V_e = \frac{V_i}{\sqrt{1 + \frac{fR}{12K^2(1 + \phi_{ent})} \left(1 + \frac{4 \frac{K\sqrt{L_e} - 1}{R}}{\left(1 + \frac{K}{R}\sqrt{L_e} \right)^4} \right)}} \quad (6)$$

Equation (6) is the general solution for fluidity of a pure metal, or any metal that freezes in a "plane front" manner, poured at the freezing temperature. Equation (6) may be solved numerically and has been solved for the conditions of the experimental approach which are set forth as conditions for analysis in Appendix E. The comparison between experimental and analytical results is shown in Figure 1.

Case with Superheat - Pure Metal

In general, there are four zones in the length of a fluidity test:

1) the zone where no freezing ever occurs due to superheated metal, 2) the zone where freezing once occurred but where superheated metal has caused remelting so that no solid remains, 3) the zone where solid metal exists but where remelting is occurring, and 4) the zone where solidification is progressing. In flow analysis when turbulent flow is present, zone (3) is assumed to be small, that is, the mixing of turbulent superheated metal with solid metal is expected to eliminate either the superheat or the solid very rapidly. Neglecting zone (3) and realizing that zones (1) and (2) are identical from a friction-loss standpoint, equation (2) becomes:

$$\frac{dL_e}{d\theta} = V_e = \frac{V_i}{\sqrt{1 + \frac{fR^4}{2(1+\phi_{ent})} \left[\frac{L_1}{R^5} + \int_{L_1}^{L_e} \frac{dL}{r^5} \right]}} \quad (7)$$

where L_1 is the distance from the channel entrance to the beginning of solid metal.

Substituting equation (5) in (7) and integrating yields:

$$\frac{dL_e}{d\theta} = V_e = \frac{V_i}{\sqrt{1 + \frac{fR^4}{2(1+\phi_{ent})} \left[\frac{L_1}{R^5} + \frac{1}{6K^2R^3} + \frac{4K\sqrt{L_e-L_1} - R}{6K^2(R-K\sqrt{L_e-L_1})^4} \right]}} \quad (8)$$

Unfortunately, to evaluate (8) an extremely laborious numerical procedure is required. Equation (7) must first be solved to determine how L_1 and K are related to θ , L_e , and/or V_e .

Case with Superheat - Alloys

Certainly no quantitative analysis of fluidity of alloys may be made unless the mechanism of freezing can be put in quantitative terms. A rough analysis of the effect of superheat on the fluidity may be made, however.

Fluidity is composed of Zones I, II, and IV since Zone III has been shown to be small. Zone I may be calculated by use of 1) equations (1) and (4), 2) a simple relation expressing the loss in temperature of liquid metal per unit length:

$$\Delta Q = \rho c \pi R^2 \Delta T \quad (9)$$

and 3) assuming that there is no heat convection or conduction longitudinally relative to the metal, that is the heat content of the metal travels with the average metal velocity by convection and radially toward the mold by convection and conduction. The details of the analysis are in Appendix G. The result is that fluidity should increase 0.227 cm for each degree of superheat for R equal to 0.193 cm. The minimum slope (and thus minimum Zone II) of the fluidity versus superheat curves for this tube size is 0.178 (see Figure J1). Zone IV is assumed to be constant (see Figure 10). The discrepancy is accounted for largely by the inaccuracy of the third assumption above and by the use of small values for the computations in Appendix G.

V EXPERIMENTAL APPROACH

Apparatus

The apparatus for measuring fluidity was essentially the same as that used by Ragone⁴³, the vacuum fluidity tester. This tester was chosen because of the excellent control over the applied pressure and metal temperature. Modifications included a solenoid valve wired with a telechron timer so that pressure could be applied as consistently as possible and so that an accurate record of distance and time could be recorded on movie film. A schematic sketch of the apparatus is shown in Figure 2.

The mold channel consisted of glass tubes specially chosen for their dimensional accuracy, ± 0.002 -inch inside diameter. The tube sizes chosen were:

<u>Tube</u>	<u>Inside Diameter</u>	<u>Wall Thickness</u>
"5 mm"	0.386 cm	0.093 cm
"7 mm:	0.483 cm	0.103 cm

By necessity the tubes had to be bent so they could reach the metal. This bend, even though done very carefully and purposely made to a large radius (about 6 inches), caused the inside diameter at the bend to become somewhat reduced causing small variations in frictional resistance and also variations in freezing time due to the smaller cross-sectional area.

In order to simplify heat flow analysis a tube with a large wall thickness was desired to insure that the heat flow was always of the "infinite mold" type - that is, flow was stopped before the outside of the tube

was heated appreciably. The "infiniteness" of the tube sizes chosen is shown in Appendix H. The tubes resemble infinite molds as long as flow time does not exceed 1.5 secs for the smaller tubes and 1.8 secs for the larger tubes.

The tin-rich end of the tin-lead binary system was chosen for this study because 1) no scatter in results from surface films or dissolved gas, 2) physical data for tin, lead, and the whole binary system are better known than any other suitable metals, and 3) low melting temperatures make for better control and ease of handling.

All alloys were made from C. P. materials. Maximum impurity limits are listed in weight percent:

<u>Metal</u>	<u>Impurities</u>							
	As	Cu	Bi	Fe	Pb	Ni	Zn	Ag
Tin	.0001	.001	-	.005	.005	-	.005	-
Lead	.0001	.0003	.0001	.001	-	.001	-	.0002

Procedure

Varying Chemistry

The chemistry was varied from pure tin to 5% lead - .95% tin. The intervals were kept small at low alloy concentrations (below 2% lead) so as to be able to detect the concentration at which the "plane front" mechanism deteriorated. For each alloy a series of at least four tests were made at different temperatures. Only the small tubes were used in this series.

Varying Pressure

The pressure was varied from about 3 inches of metal head to about 30 inches of metal head for 1) pure tin in small tubes, 2) tin - 5% lead in small tubes, and 3) tin - 5% lead in larger tubes. Again each pressure

was tested over a range of temperatures except for pure tin at high pressures when the length of flow became dangerously long.

Varying Temperature

The temperature was varied between 310°C and as close to the liquidus temperature as possible.

Results

The fluidity and fluid life of all fluidity tests as a function of superheat is presented in Appendix J. In general the larger tubes seem to yield more consistent data than the small tubes. Also, the longer the fluid life, the less consistent are the results; and at fluid life above 1.5 secs there seems to be very little consistent behavior. This is in keeping with the results of the heat flow analysis.

Figure 3 shows a comparison of Ragone's results⁴² with tin and the results of this investigation. The initial slopes of the same size tubes are identical, but the fluidity of pure tin is twice that obtained by Ragone. Figure 3 also shows a comparison of 0.4% lead which coincides at the melting point with Ragone's data for a slightly smaller tube. If the curves are comparable, then the conclusion must be that Ragone used a lower grade of tin, probably commercial purity. The curves of Figure J1 show the difference that a fraction of a weight percent at low concentrations can have on fluidity.

Effect of Alloying

The data for low alloy tin, extrapolated to the liquidus temperature, are shown in Figure 4 as a function of composition. The composition is in logarithmic scale only to show better the results at very low concentrations. Between 0.1% and 1% lead a curve can easily be drawn through the fluidity

points and the fluid life points, but at 0.07% lead there is a definite discontinuity in both curves. This composition is the "critical" composition above which plane front solidification deteriorates rapidly.

There is definite evidence that the plane front mechanism is modified from 0.004% lead (C. P. tin) to 0.07% lead. This trend is shown in Figures 4, 5, and 7. But rapid deterioration does not occur til 0.07% lead. There is another discontinuity in Figure 4 at about 1% lead, although this one is not as marked as the other. Above 1% lead the fluidity changes very little with composition. This behavior is shown better in Figure 5 which presents fluidity as a function of composition. Figure 5 also shows the behavior of freezing time and the slope of the fluidity-temperature curves as a function of composition.

Varying Metal Head

The laws of fluid dynamics require that initial velocity of fluidity tests be proportional to the square root of metal head (Z). Figure 6 shows that this is true for all alloys, temperatures, and tube sizes. The initial velocity was measured from motion pictures. Much more remarkable is the excellent linear relation between fluid length and the square root of metal head (or initial velocity) as shown in Figure 6.

Figure 7 is a combined chart showing variation of fluidity with fluid life at the liquidus temperature. Composition, metal head, and tube size are parameters. All data are shown for liquidus temperature.

Motion pictures were made of all runs. Figures 8 and 1 are samples of the results of the motion picture analysis for a tin - 5.1% lead alloy in a large tube and for pure tin in a small tube respectively.

Figure 8 shows a characteristic behavior for the alloys with more than about 2% lead. The leading end of the stream separated and filled

only part of the glass tube. This leading runner of metal was sometimes over seven cm long. It often developed in the early part of those runs with metal head over ten inches; it developed in the last part of the run for most runs with under ten inches metal head. As Figure 8 shows, sometimes the runner would stop, apparently frozen, then the tube would continue to fill up in the runner section till the liquid metal ran past the old runner only to form a new runner and eventually a cascade of runners. It appears that under certain conditions this effect can propagate itself.

Discussion

Effect of Alloying

Figures 4 and 5 indicate three distinct areas of fluidity corresponding to the three areas mentioned in the Introduction. The "plane front" mechanism is located at very pure tin and little, if any, improvement in fluidity is to be expected for purer metal since the "plane front" mechanism assumes the behavior of very pure metal. Of course, it is possible to encounter undercooling effects which become more probable with purer metal, but the extreme agitation of fluidity tests would be expected to limit undercooling to negligible effects.

The critical concentration which marks the end of pure "plane front" freezing should be given by Huccke's equation¹⁷ for a condition of "perfect" stirring:

$$G_{min} = \frac{-m u c_o (1-K)}{D} \quad (10)$$

where G_{min} = minimum temperature gradient in the liquid
to maintain "plane front" interface

m = slope of liquidus

u = $\frac{dr}{dt}$, rate of advance of liquid-solid interface

c_0 = bulk solute concentration in the liquid

K = partition ratio

D = diffusion constant for solute atoms in liquid solvent

Using data for lead in tin ($m = -1.29^\circ\text{C}/\%\text{Pb}$ ³¹, $(1 - K) = .9344$, $D = 3 \cdot 10^{-5} \text{ cm}^2/\text{sec}$ ⁴⁹), assigning a value of 0.1 cm/sec for u (the value found using the data of Appendix F), and using 0.07% for c_0 gives a liquid temperature gradient of $28.4^\circ\text{C}/\text{mm}$. This figure could be low due to 1) imperfect stirring, 2) c_0 actually higher than 0.07% which could be true at any point downstream from freezing metal which is rejecting lead. This value of G_{min} may be further inaccurate due to uncertainty of D at 232°C for the concentration of lead involved. (Ref. 49 gives $D = 3.7 \cdot 10^{-5} \text{ cm}^2/\text{sec}$ at 500°C .) It seems that equation (10) will not be conclusive in supporting the statement that plane front freezing breaks down at about 0.07% lead until data is better established and until the effect of temperature gradient in the liquid on solidification processes is established.

Figure 9 shows the effect of alloy additions on the dynamics of the metal stream at only a few degrees superheat (6° to 8°C). It can be seen that no radical change in dynamics occurs before 0.092% lead, but above this content, the stream stops very suddenly. This behavior has also been shown by Feliu¹³ with aluminum-tin alloys. A sudden stop can be explained by a mechanism which provides for the formation of dendrites which flow downstream and eventually cause enough friction to stop the flow. Lips and Nipper²⁷ have described this mechanism. Another mechanism provides for the sudden growth of stationary dendritic needles reaching into the metal stream - conditions for this net of dendrites are more favorable with a wide temperature range of freezing. The former mechanism theoretically stops the flow only at the tip of the stream, the latter conceivably could stop the stream some distance back from the tip.

The separation of the tip from the glass wall, observed in many of the 5.1% lead alloys, is not possible with the mechanism of moving dendrites, but is possible with the stationary dendrites or a combination of the two.

Above about 1% lead the fluidity at the melting point does not change (see Figure 5). In fact there is very little change in the points on the L_f versus θ_f plot, Figure 7. As mentioned in the Results section of this paper, there is not expected to be much change in this region of the phase diagram until the effects of the eutectic are felt.

By use of equation 1 and the distance versus time curves from the motion pictures, it was possible to graphically find the heat removed through each part of the mold prior to time of freezing as a function of distance along the mold. These curves were then graphically integrated to find total energy removed from the metal. These values are plotted for 5.1% lead alloy in small tubes in Figure 11 as a function of superheat for three values of metal head. By extrapolation the total energy removed for fluidity tests at the liquidus was found. This may be compared with the total energy of fusion in the length of the fluidity test.

<u>Z</u>	<u>Energy Removed</u>	<u>Energy of Fusion</u>	<u>Ratio</u>
10 in	48.5 cal	310 cal	0.1565
6	36.5	192	0.19
3.5	29	161	0.18

This ratio is very close to the 0.2 ratio which Klyachko and Kunin¹⁸ used as the empirical ratio for alloys.

Effect of Superheat

The effect of superheat is shown in Figure 5 where $\frac{dL_f}{dT_i}$ is plotted. This slope (measured at the liquidus) varies almost identically with the fluidity and the fluid life (see Figure J5). As mentioned in the Introduction,

a long fluid life allows for a maximum of decrease in heat flow rate which gives superheated metal an opportunity to affect more and more of the fluidity length. In effect Zone II, the zone where complete remelting of solid metal occurs, is much larger with longer fluid life. Schematically this effect is shown in Figure 10.

Effect of Metal Head

The effects of metal head are shown in detail in Appendix J and are compiled for tin and tin-lead alloys at the liquidus temperature in Figures 6 and 7.

Figure 6 shows the linear variation of initial velocity with the square root of metal head, a relation which was expected from hydrodynamic analysis.

Linear variation of fluidity with initial velocity for pure tin and for 5.1% lead alloy in both size tubes is shown in Figure 6. In Figure 7 the same alloys show practically no variation in fluid life. The only conclusion that can be drawn is that velocity of the fluid has no effect on the freezing time at the point in the metal stream where freezing causes cessation of flow. Logically, if the moving dendrite mechanism controls the fluid life by accumulating dendrites at the leading end, then a rapid stream will have shorter life than a slow stream. On the contrary, fluid life being independent of stream velocity indicates that the controlling mechanism is one wherein the dendrites remain stationary, attached to the mold wall. This mechanism requires that freezing of the stream occur first at a point near the entrance to the fluidity mold where the most solid should have formed provided, of course, that there is no superheat. Using equation (1) and the freezing times from Figure 7, Q_s of 3.15 cal and 4.8 cal were found for the small and large tubes respectively. These energies correspond to about 25% solid in each case.

VI CONCLUSIONS

From Analytical Approach:

1. General equations for heat flow and fluid flow may be applied to fluidity of pure metals, but usually the result is not easily integrable.
2. In molds with low heat conductivity, eg. glass and sand, the shape of the liquid-solid interface for pure metals has been found to be parabolic, where the latus rectum is a function of stream velocity and test conditions.
3. In alloys or pure metals the effect of superheat is two-fold. That part associated with initial cooling to the melting point (Zone I) may be approximated. The second part associated with remelting of solid metal (Zone II) is more difficult to analyze.

From Experimental Approach:

1. As more lead is added to tin, the character of fluidity passes through three stages which are separated by critical compositions. The first stage (up to about 0.1% lead) is that of pure or nearly pure metal characterized by "plane front" freezing, high fluidity, and long fluid life - there is little, if any, improvement in fluidity with purer tin. The second stage sees the break down of "plane front" freezing accompanied by rapid decrease in fluidity and fluid life. The third stage (over about 1% lead) is characterized by very low fluidity and fluid life and a "net dendritic" mechanism. Again the fluidity does not change with changing composition up to 5% lead.

2. The effect of superheat parallels the curves of fluid life (and/or fluidity). The second section (Zone II) where remelting occurs depends on fluid life - the longer the fluid life, the larger is Zone II.

3. For alloys of over 1% lead in tin:

The fluid life at the liquidus is very small and does not change with varying initial velocity.

The cessation of flow is very rapid and often accompanied by separation of the metal stream at the tip due to inertia.

The mechanism of freezing seems to be one characterized by "net dendrites" choking the stream near the mold entrance. The amount of solid near the mold entrance at the moment of cessation of flow was calculated to be 25% of the volume.

SUGGESTIONS FOR FUTURE WORK

1. Other metallic binary eutectic systems should be investigated to determine the applicability of the "net dendritic" mechanism to other alloys. A plot of L_f versus θ_f , or a comparison of the percent solid at the freeze-off point, would give an indication of changes in the mechanism.
2. Detailed knowledge of the mechanism of solidification is still lacking. Experiments should be developed to more firmly establish the mechanism.
3. The point of breakdown of the "plane front" freezing should be investigated for other alloy systems.
4. A good method for solving equations for elements of fluidity is by use of a computer. Detailed effects resulting from parameter changes could be presented in the form of families of curves.

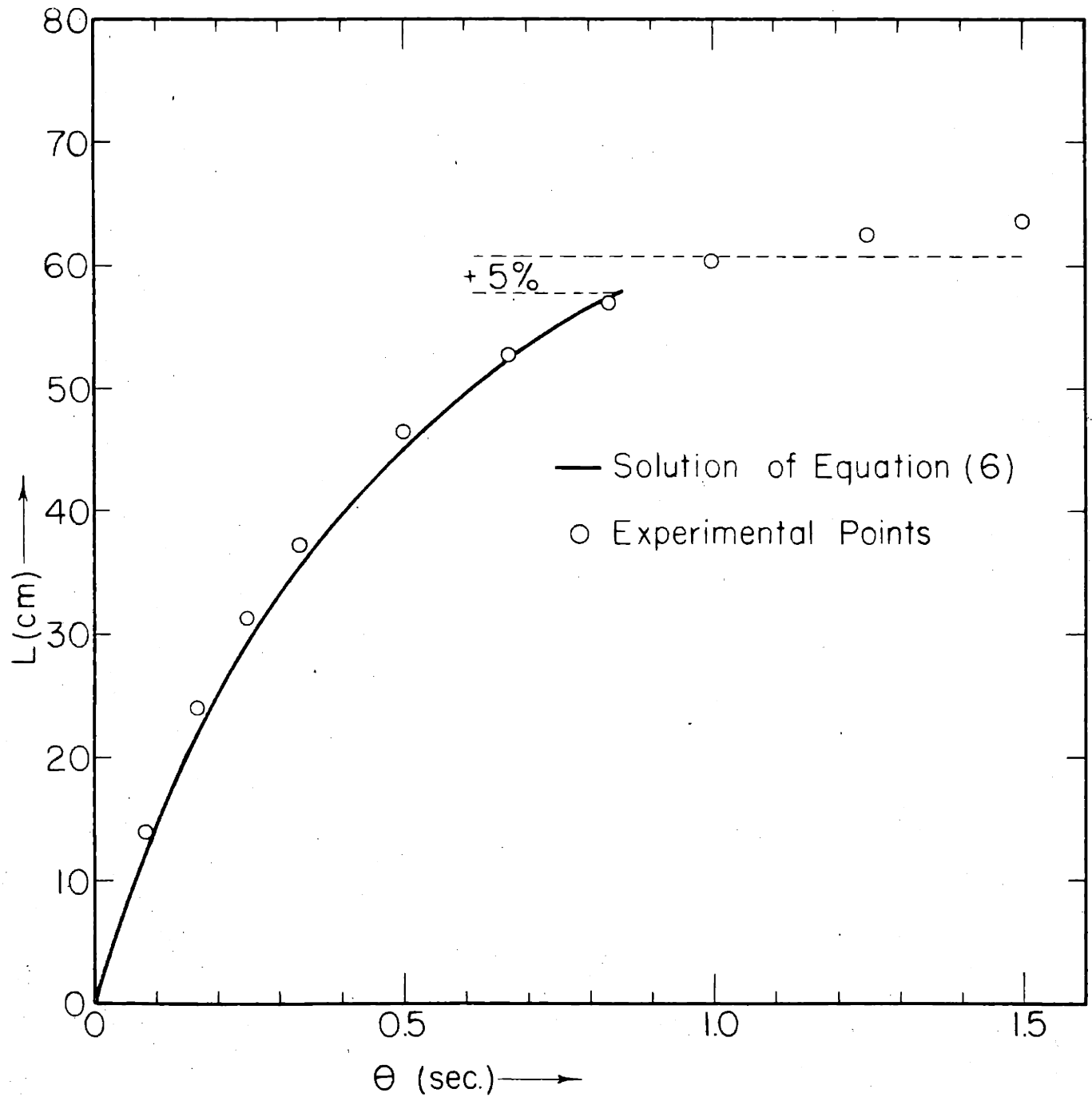


FIG.1 CURVES OF FLUIDITY VERSUS TIME COMPARING ANALYTICAL (EQUATION 6) TO EXPERIMENTAL

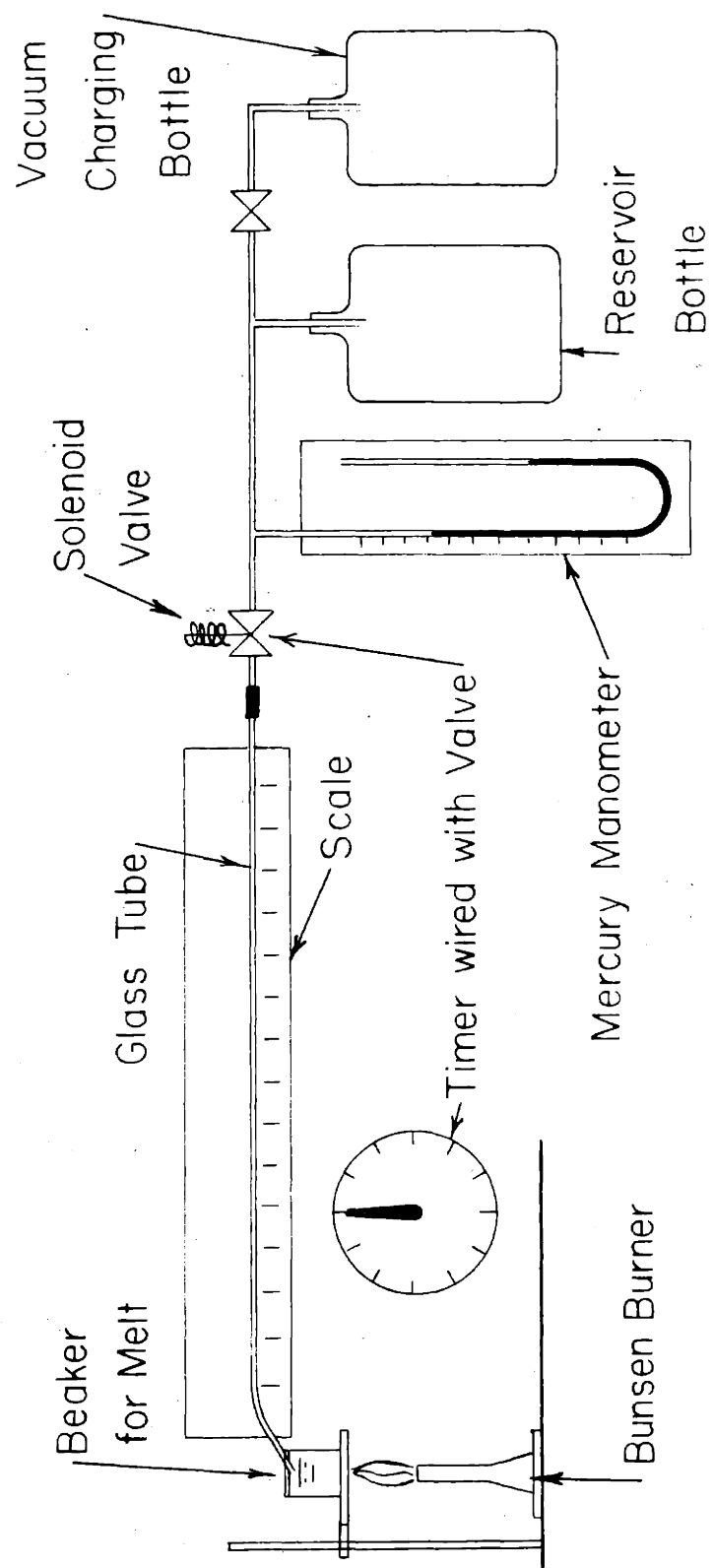


FIG. 2 SCHEMATIC SKETCH OF VACUUM FLUIDITY APPARATUS

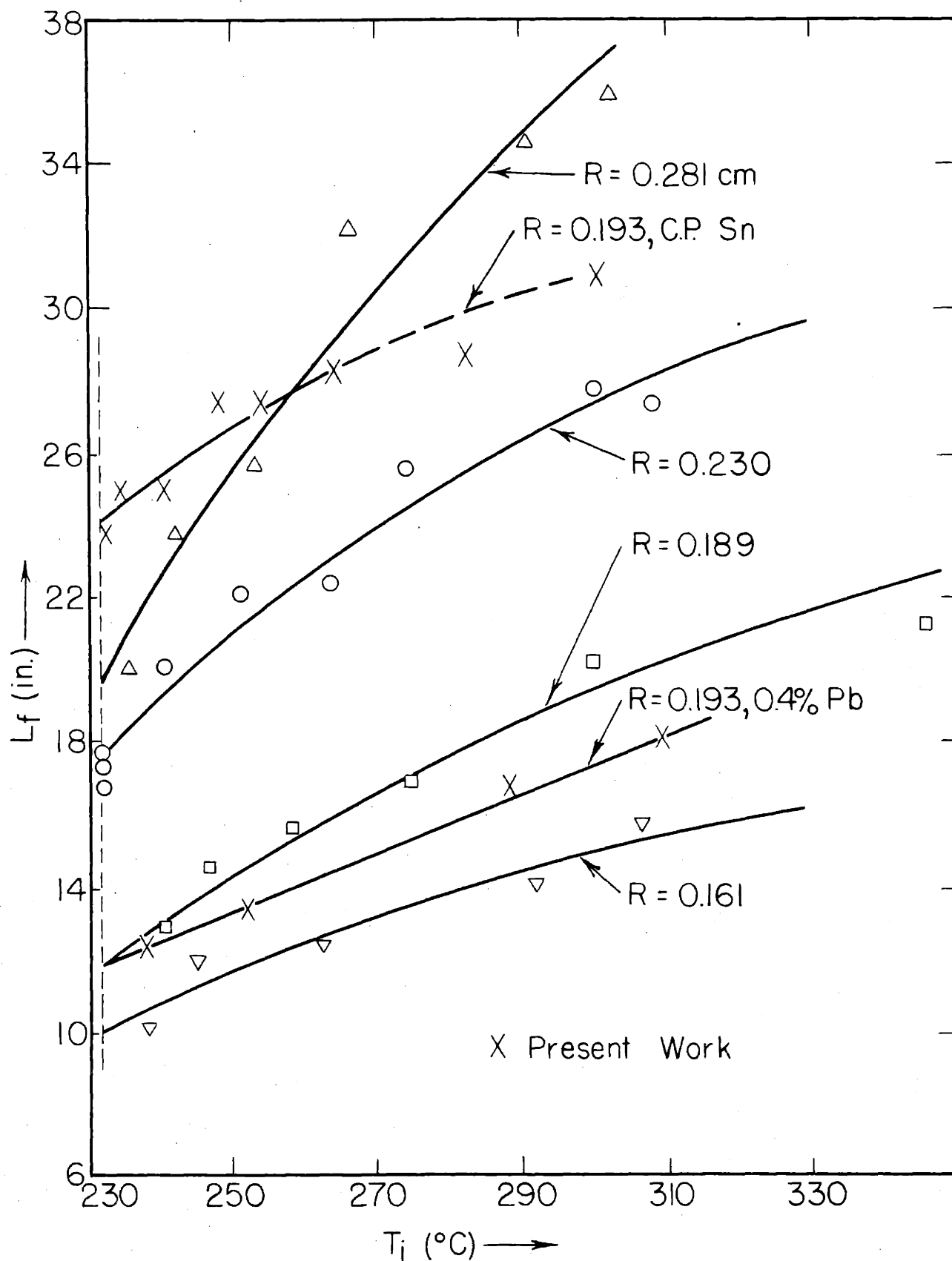


FIG. 3 COMPARISON FLUIDITY OF PURE TIN WITH DATA FROM RAGONE

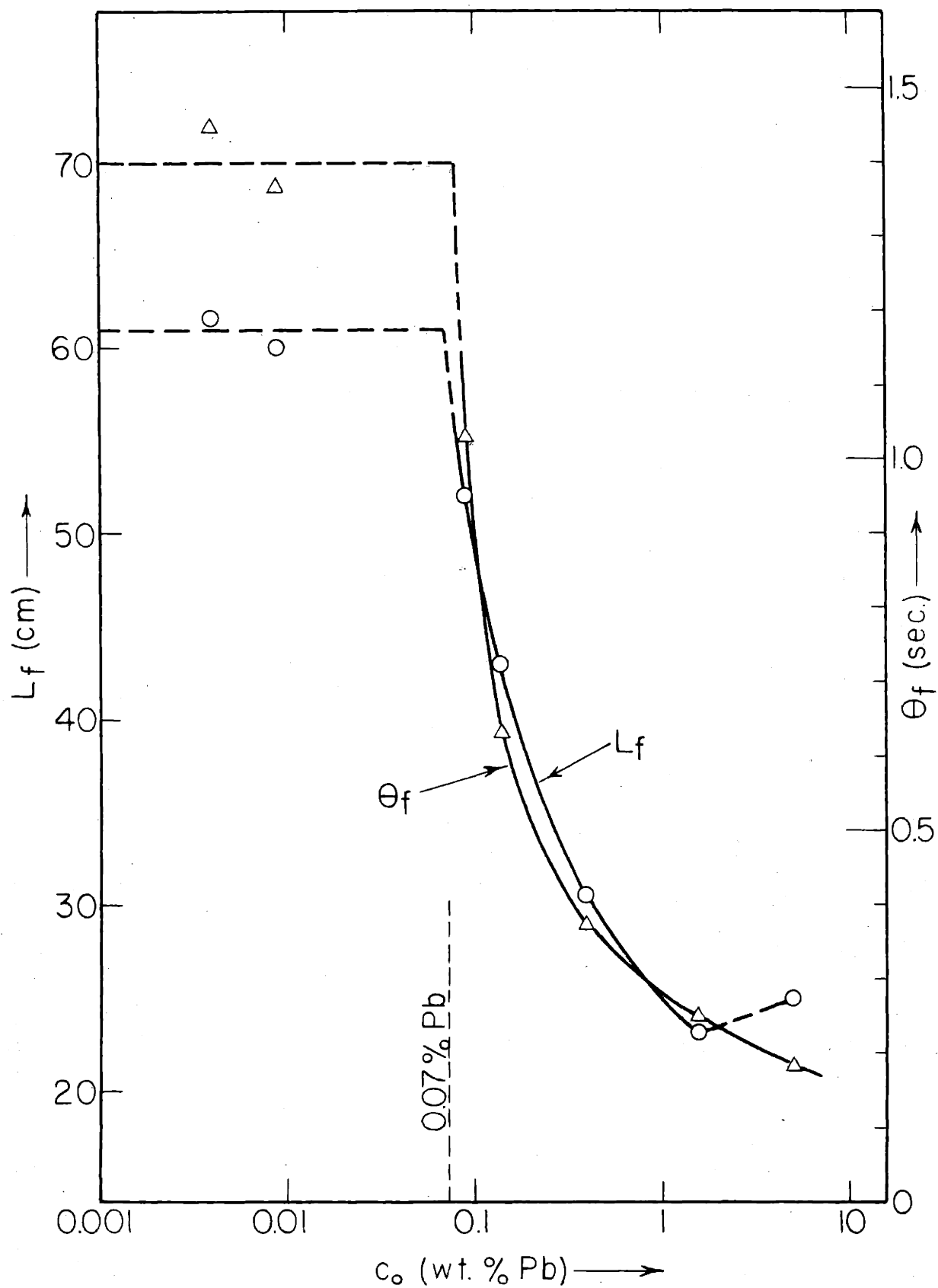


FIG. 4 FLUIDITY AND FLUID LIFE AS A FUNCTION OF LOG COMPOSITION

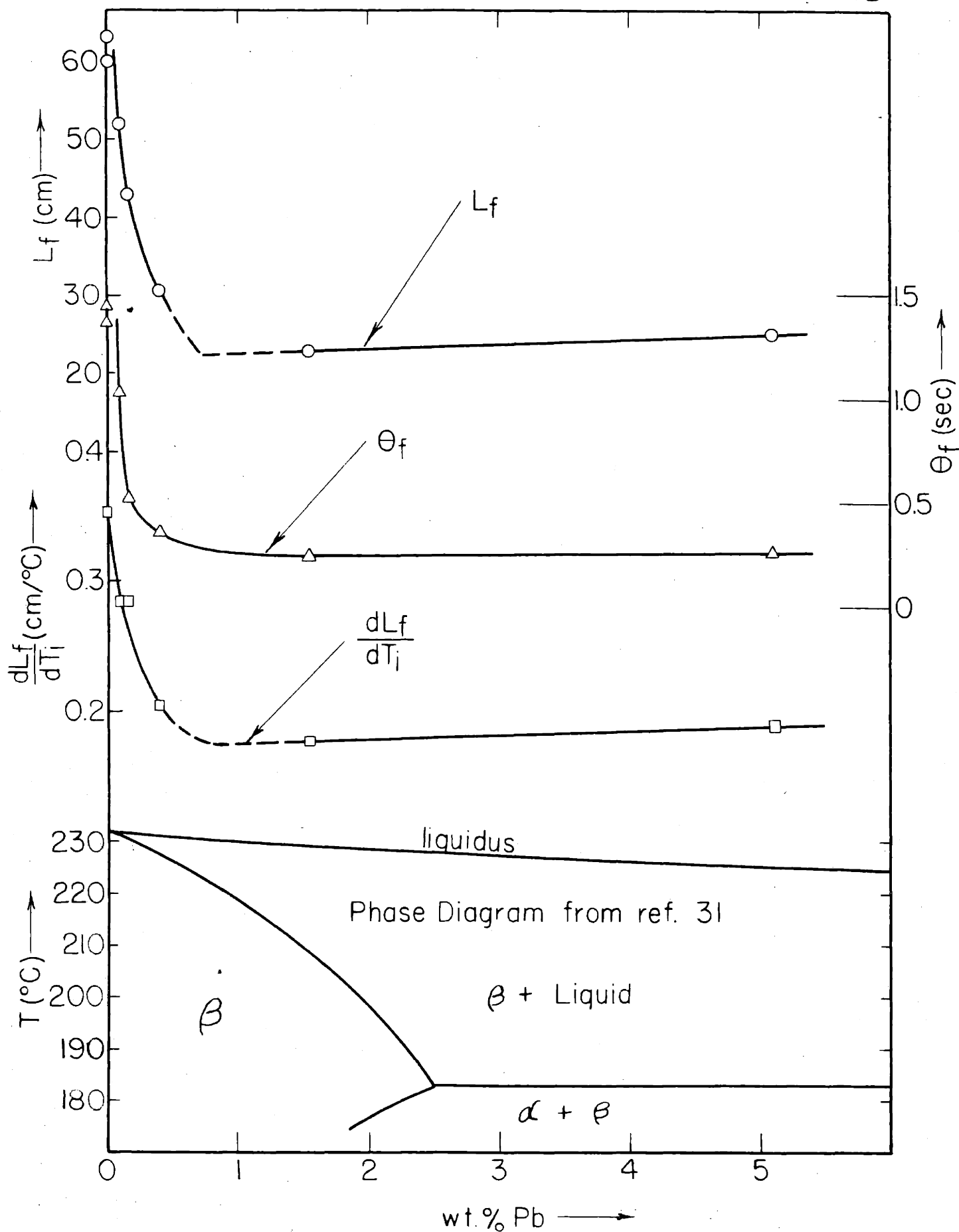


FIG. 5 FLUIDITY, FLUID LIFE, AND SLOPE OF FLUIDITY-TEMPERATURE CURVES AS A FUNCTION OF COMPOSITION AT LIQUIDUS TEMPERATURE

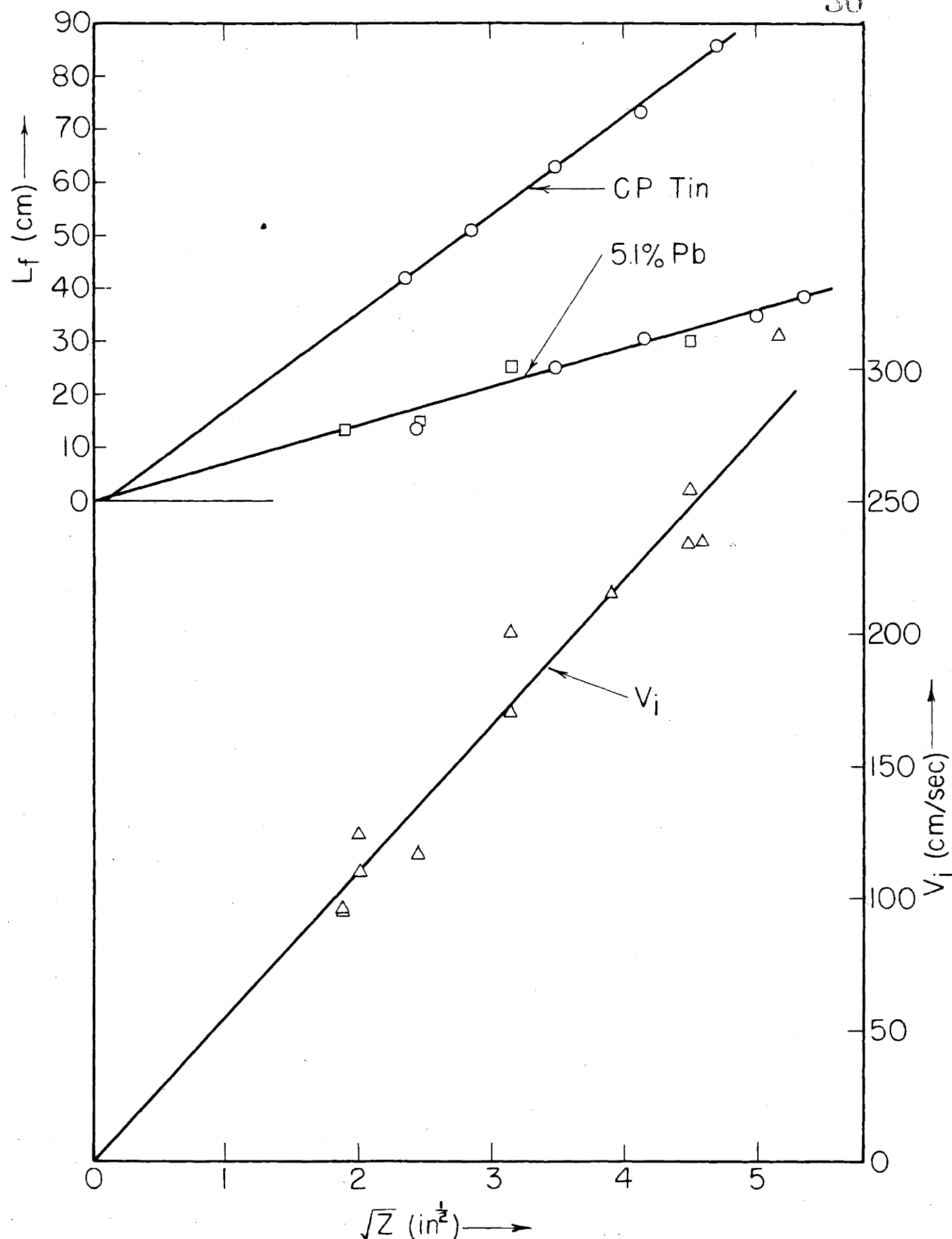


FIG. 6 FLUIDITY AND INITIAL VELOCITY AS FUNCTIONS OF THE SQUARE ROOT OF METAL HEAD

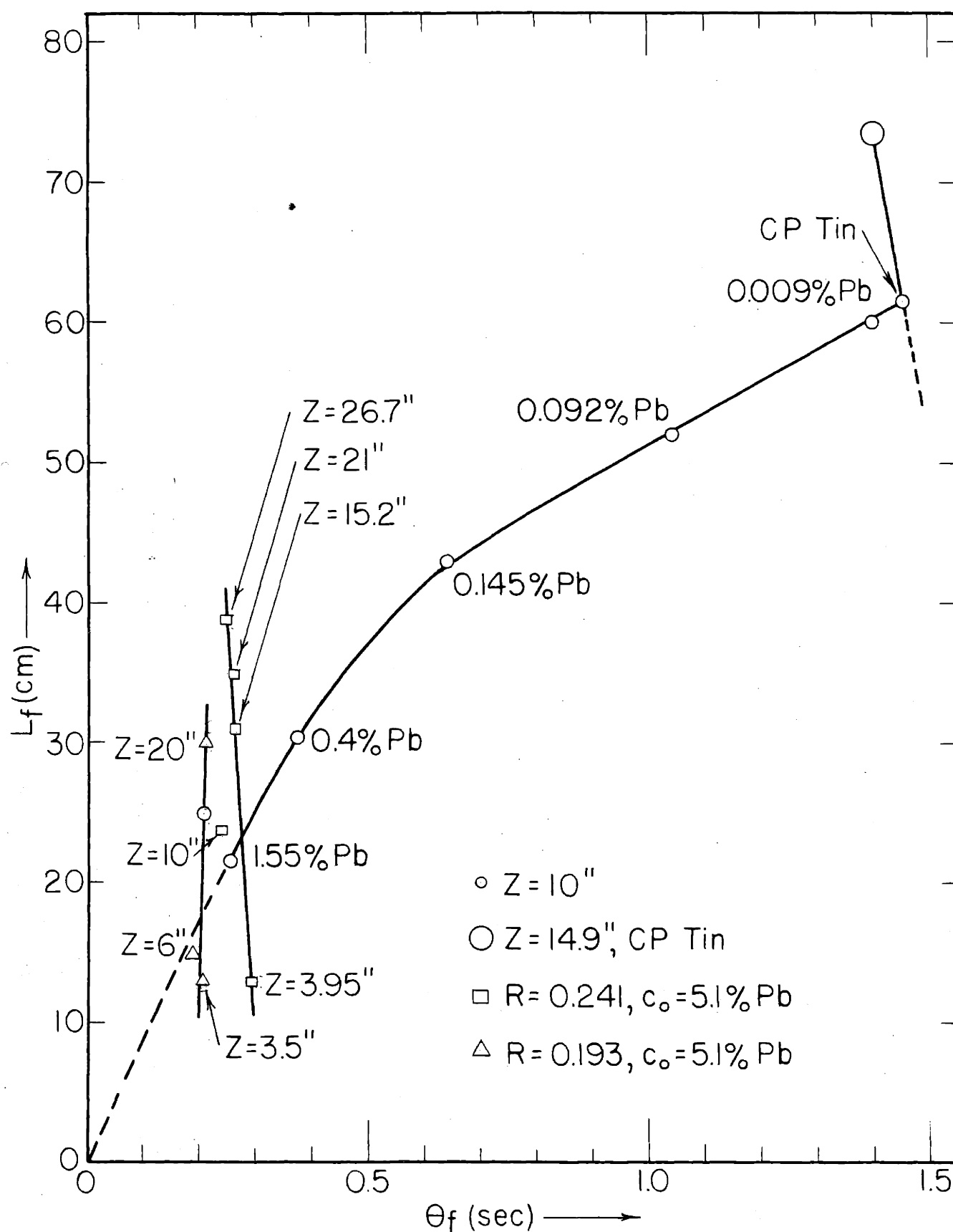


FIG. 7 FLUIDITY AS A FUNCTION OF FREEZING TIME FOR VARIOUS METAL HEADS AND ALLOYS AT LIQUIDUS TEMPERATURES

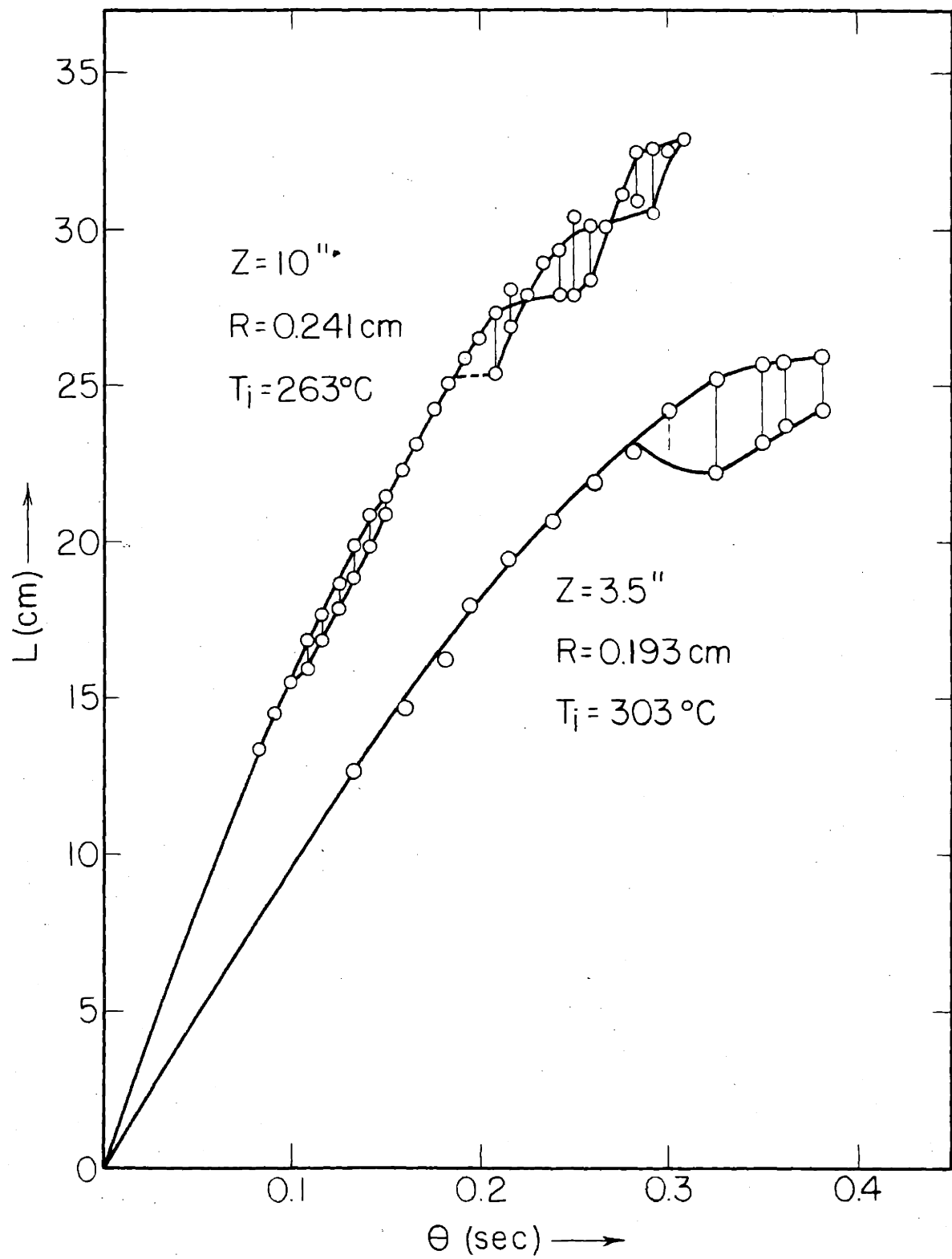


FIG. 8 DISTANCE AS A FUNCTION OF TIME FOR TIN - 5.1% LEAD ALLOYS

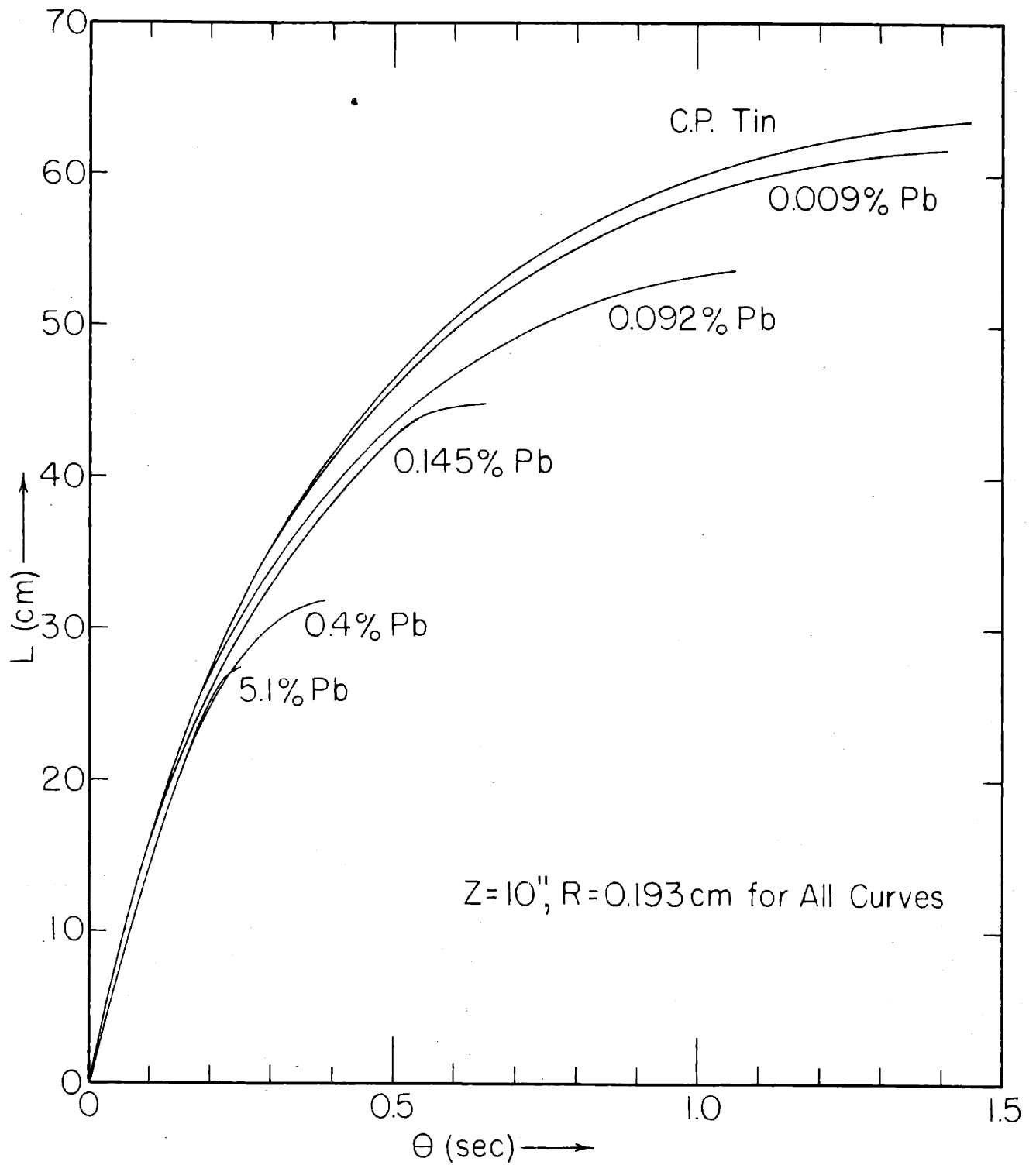


FIG. 9 DISTANCE VERSUS TIME FOR TIN-LEAD ALLOYS AT 240°C

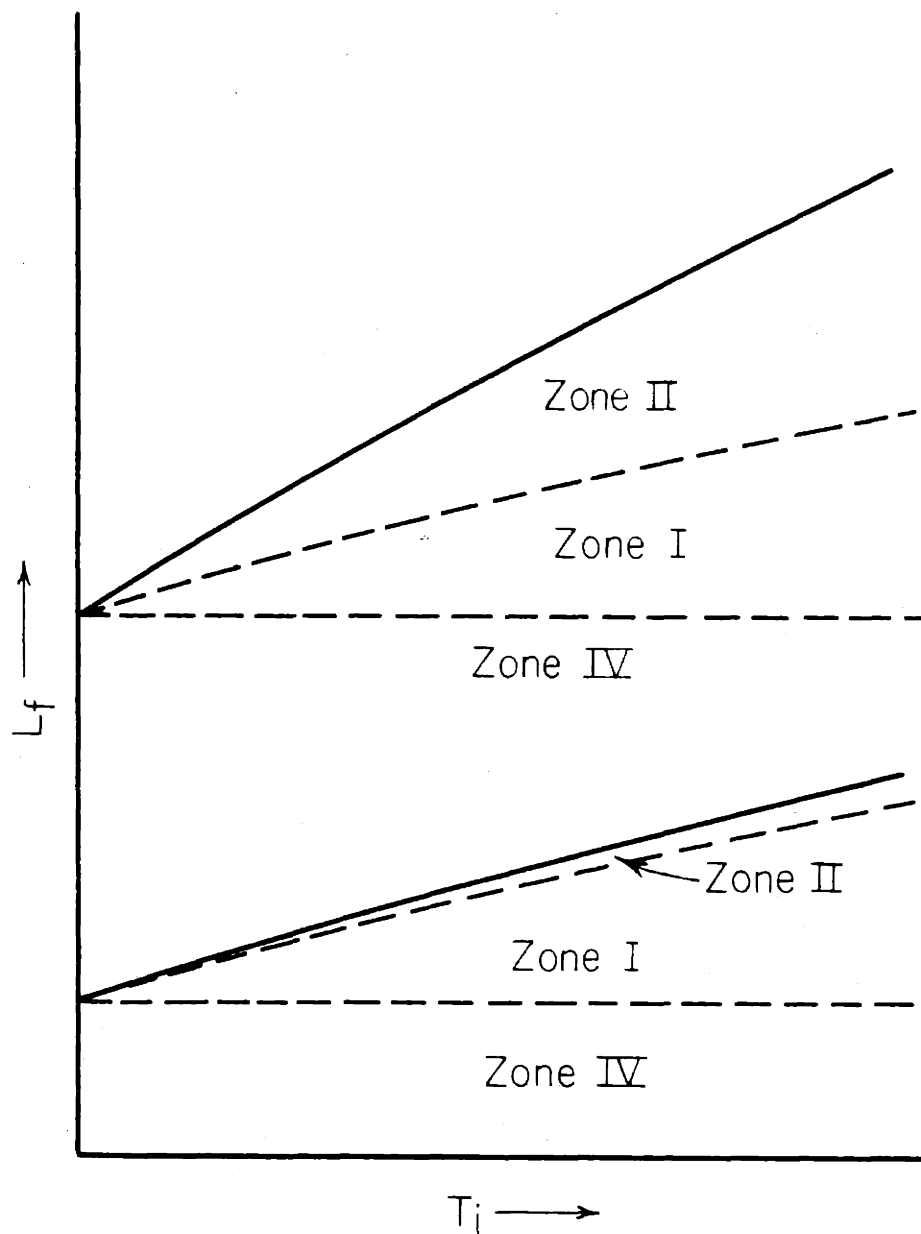


FIG. 10 SCHEMATIC CURVES SHOWING THE INCREASED INFLUENCE OF ZONE II WITH INCREASED FLUIDITY

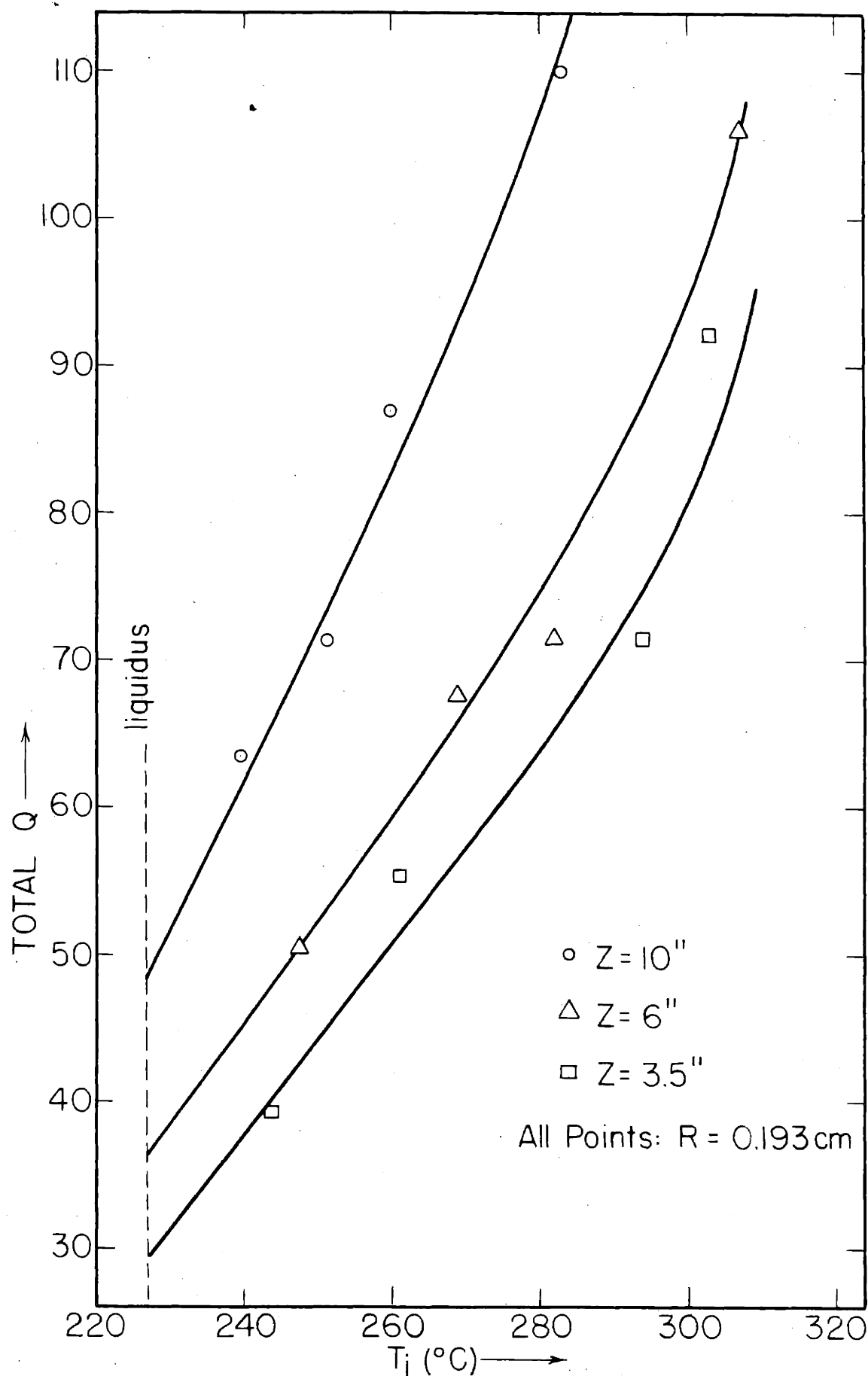


FIG. 11 TOTAL ENERGY REMOVED FROM METAL PRIOR TO CESSATION OF FLOW FOR 5.1% LEAD ALLOYS

BIBLIOGRAPHY

1. Adams, C.M., "Thermal Considerations in Freezing", Liquid Metals and Solidification, American Society for Metals, Cleveland, Ohio, 1958.
2. Andrew, J.H., Bottomley, G.T.C., Maddocks, W.R., and Percival, R. T., "The Fluidity of Alloy Steels", Iron and Steel Institute, Special Report No. 23, 1938, pp. 5-34.
3. Andrew, J.H., Percival, R. T., and Bottomley, G. T. C., "The Fluidity of Iron-Carbon and Other Iron Alloys", Iron and Steel Institute, Special Report No. 15, 1936, pp. 43-64.
4. Ash, E. J., "Malleable Iron Castability Test", Trans., A.F.A., 1939, vol. 47, pp. 609-617.
5. Briggs, C.S., "The Fluidity of Metals", Metals Handbook, pp. 199-204, American Society for Metals, Cleveland, Ohio, 1948.
6. Clark, K.L., "Fluidity Testing of Foundry Alloys", Trans., A.F.A., 1946, vol. 54, pp. 37-48.
7. Courty, A., "Contribution a l'etude de la Coulabilite", Revue de Metallurgie, 1931, vol. 28, no. 3, pp. 169-182 and vol. 28, no. 4, pp. 194-208.
8. Desch, C.H., "Physical Factors in the Casting of Metals", Foundry Trade Journal, April-June 1937, vol. 56, pp. 505-508.
9. DeVries, Ind. Eng. Chem., 1930, vol. 22, p. 617.
10. Dow Chemical Company, "Viscosity of Liquid Magnesium", (unpublished).
11. Eastwood, L.W. and Kempf, L.W., "Measurement of Fluidity of Aluminum Casting Alloys", Trans., A.F.A., 1939, vol. 47, pp. 572-582.
12. Evans, E.P., "The Fluidity of Molten Cast Iron", Journal of Research and Development, British Cast Iron Research Association, 1951, vol. 4, no. 2.
13. Feliu Matas, S., M.I.T., (unpublished).

14. Fisher, H. J. and Phillips, A., "Viscosity and Density of Liquid Lead-Tin and Antimony-Cadmium Alloys", Journal of Metals, September 1954.
15. Greaves, R. H., "Fluidity of Steel in Relation to Method of Manufacture, Composition, and Temperature of Casting", Iron and Steel Institute, Special Report No. 23, 1938, pp. 5-34.
16. Hildebrand, Duschak, Foster, and Beebe, Journal of American Chemical Society, 1917, vol. 39, p. 2293.
17. Hucke, E. E., "Factors Affecting the Mode of Solidification of Alloys in a Controlled Freezing System", Sc. D. Thesis, Dept. of Metallurgy, M. I. T., 1953.
18. Klyachko, Yu. A. and Kunin, L. L., "Fluidity of Metals and Methods of Determining Fluidity", (Brutcher Trans. 2539), Zavodskaya Laboratoriya, 1949, vol. 15, no. 10, pp. 1198-1206.
19. Kondic, V., "Liquid Metal Properties", Foundry Trade Journal, June 1950, vol. 88, pp. 691.
20. Kondic, V., "Fluidity Testing Developments", Foundry Trade Journal, January 1956, vol. 100, pp. 31-36.
21. Kondic V. and Kozlowski, H. J., "Fundamental Characteristics of Casting Fluidity", Journal of Institute of Metals, 1949, vol. 75, pp. 665-678.
22. Kron, E. C., and Lorig, C. H., "The Flowability of Cast Steel", Trans., A. F. A., 1939, vol. 47, pp. 583-608.
23. Krynitsky, A. I., "Progress Made in Fluidity Testing of Molten Metals During the Last Ten Years", Trans., A. F. S., 1953, vol. 61, pp. 399-411.
24. Krynitsky, A. I., "Surface Tension of Molten Metals", Metals and Alloys, 1933, vol. 4, p. 79.
25. Kunin, L. L., "Apparatus for Determinations of Fluidity and Rate of Flow of Molten Metal", (Brutcher Trans. 2516), Zavodskaya Laboratoriya, 1949, vol. 15, pp. 870-872.
26. Lillieqvist, G. A., "Influence of Temperature on Fluidity and Surface Appearance of Steel Castings", Trans., A. F. S., 1950, vol. 58, pp. 261-269.
27. Lips, E. and Nipper, H., "Untersuchungen uber den Einfluss der Kristallausscheidung auf die Flieseigenschaften von Schmelzen", Die Giesserei, July 1938, vol. 25, pp. 369-372.
28. Liquid Metals Handbook, Atomic Energy Commission, Dept. of the Navy, Washington, D. C., June 1950.

29. McAdams, Heat Transmission, McGraw-Hill Book Company, Inc., New York, 1942.
30. Meade, D., "Fluidity of Some Aluminum Alloys", S. M. Thesis, Department of Metallurgy, M. I. T., June 1958.
31. Metals Handbook, American Society for Metals, Cleveland, Ohio, 1948.
32. Moody, L. F., "Friction Factors for Pipe Flow", Trans., ASME, 1944, vol. 66, pp. 671-684.
33. Niesse, J. E., Flemings, M. C., and Taylor, H. F., "Fluidity of a Series of Magnesium Alloys", Trans., A. F. S., vol. 65, 1957.
34. Perin, S. and Berger, R., "A Contribution to the Study of Fluidity of Cast Iron," Trans., A. F. A., 1934, vol. 42, pg. 589.
35. Porter, L. P. and Rosenthal, P. C., "Factors Affecting Fluidity of Cast Iron", Trans., A. F. S., 1952, vol. 60, pp. 725-735.
36. Portevin, A. and Bastien, P., "Coulabilite des Alliages, Relation avec L'Intervalle de Solidification", Comptes Rendus, 1932, vol. 194, pp. 850-853.
37. Portevin, A. and Bastien, P., "Facteurs Principaux de la Coulabilite des Metaux Purs", Comptes Rendus, 1932, vol. 194, p. 599.
38. Portevin, A. and Bastien, P., "Capillarity as a Factor in Foundry Practice", Proc. Inst. Brit. Foundrymen, 1935-36, vol. 29, pp. 88-116.
39. Portevin, A. and Bastien, P., "La Resistance Mechanique de la Peau d'Alumine et son Influence sur la Tension Superficielle du Metal Fondu", Comptes Rendus, 1936, vol. 202, pp. 1072.
40. Prussin, S. A. and Fitterer, G. R., "Some Requirements for Successful Fluidity Testing", Trans. A. F. S., 1958, vol. 66, pp. 143-149.
41. Rabinovich, Ye. Z., "On the Formulas for the Coefficient of Resistance in the Movement of Molten Metals", (Brutcher Trans. no. 2010), Doklady Akademii Nauk SSSR, 1946, vol. 54, no. 5, pp. 395-397.
42. Ragone, D. V., Adams, C. M., and Taylor, H. F., "Some Factors Affecting Fluidity of Metals", Trans., A. F. S., 1956, vol. 64, pp. 640-652.
43. Ragone, D. V., Adams, C. M., and Taylor, H. F., "A New Method for Determining the Effect of Solidification Range on Fluidity", Trans., A. F. S., 1956, vol. 64, pp. 653-657.

44. Rightmire, B.G. and Taylor, H.F., "The Fluidity of Molten Steel", Journal of Iron and Steel Institute, October 1953, vol. 175, pp. 167-176.
45. Ruff, W., "Running Quality of Liquid Malleable Iron and Steel", Iron and Steel Institute, Carnegie Scholarship Memoirs, 1936, vol. 25, pp. 1-39.
46. Saeger, C.M. and Ash, E.J., "Properties of Gray Cast Iron as Affected by Casting Conditions", Trans., A.F.A., 1933, vol. 41, p. 449.
47. Saeger, C.M. and Krynitsky, A.L., "A Practical Method for Studying the Running Quality of a Metal Cast in Foundry Molds", Trans., A.F.A., 1931, vol. 39, pp. 513-540.
48. Sarjent, R.J., and Middleham, T.H., "Fluidity-Temperature Relations of Cast Steels of Various Compositions", Iron and Steel Institute, Special Report No. 23, 1938, pp. 45-60.
49. Smithells, C.J., Metals Reference Book, Second Edition, Interscience Publishers, Incorporated, New York, 1955.
50. Stephens, Phil. Mag., vol. 14, 1932, p. 897.
51. Taylor, H.F., Rominski, E.A., and Briggs, C.W., "The Fluidity of Ingot Iron and Carbon and Alloy Cast Steels", Trans., A.F.A., September 1941, vol. 49, no. 1, pp. 1-93.
52. Walker, T.R., "Works Results Using the Ruff Fluidity Test", Iron and Steel Institute, Special Report No. 23, 1938, pp. 34.
53. West, T.D., Metallurgy of Cast Iron, Cleveland Printing Co., Cleveland, Ohio, 1902.
54. Worthington, J.E., Foundry Trade Journal, July 27, 1950, vol. 87, p. 87.
55. Zeigler, N.A., and Northrup, H.W., "Effect of Superheating on Castability and Physical Properties of Cast Irons", Trans., A.F.A., 1939, vol. 47, pp. 620-652.

APPENDIX A

QUANTITATIVE ANALYSES IN THE LITERATURE

Few theoretical analyses of metal flowing and freezing in a mold have been rigorously made. The history is as follows:

First investigators to arrive at an explanation for fluidity were Portevin and Bastien³⁶ who said that fluidity was a product of average velocity and fluid life (time before freezing-off). They derived:

$$L_f = a \frac{c\rho(T_i - T_m)}{T_m - T_r} + b \frac{\rho H}{T_m - T_r} \quad (A1)$$

where the first term represents velocity (incorporated in constant a) and time prior to any solidification and the second term represents velocity (in constant b) and fluid time during solidification. However, equation (A1) soon proved too simple in that L_f did not depend on $(T_i - T_m)$ and H in the predicted manner.

Klyachko and Kunin¹⁸ in 1949 reviewed Russian work on methods of determining fluidity. Essentially these analyses are extensions of equation (A1). B.D. Khakhalin assumed that flow ceased when a characteristic quantity of metal crystals was suspended in the liquid. He derived equation (A2).

$$L_f = \frac{71(2R)^{5/3} H_g \mu^{7/3}}{(4ab)^{4/3}} \left[\frac{c\rho(T_i - T_m)}{T_m} \right]^{4/3} + \frac{18(2R)^2}{4ab} \left(\frac{\rho H_g}{\mu} \right)^{1/2} V_s \frac{\rho H}{T_m} \quad (A2)$$

where H_g = hydrostatic head minus head due to surface tension

a , b , and n are constants

V_s = quantity of suspended crystals (fraction of total heat of fusion)

Then Nekhendzi and Samarin assumed that flow ceases when a definite quantity of solid phase exists; this quantity being characteristic of the metal. They derived:

$$L_f = A \rho \frac{c(T_i - T_o) + H_1}{T_a - T_r} \quad (A3)$$

where T_a = average metal temperature between T_i and T_o

A = constant

H_1 = latent heat of that quantity of solid required to yield zero fluidity

Using equation (A3) Klyachko and Kunin derived equation (A4).

$$L_{f \text{ rel}} \equiv \frac{L_f}{L_{fH}} = \frac{K}{K+c} + \frac{c}{H(K+c)} (T_i - T_o) \quad (A4)$$

where $L_{f \text{ rel}}$ = "relative fluidity"

L_{fH} = "unit fluidity" or fluidity when superheat is numerically equal to latent heat ($T_i - T_o = H$)

K = fraction of latent heat required to yield zero fluidity ($K = H_1/H$)

Using equation (A4) and actual fluidity points, Figure A1 was constructed. From this graph it was concluded 1) that $K = .2$ applies at low superheat, 2) for Zn which crystallizes with highly developed dendrites $K = .2$ fails to apply, and 3) at high superheat, when proximate order is apparently

disturbed, fluidity no longer varies linearly with superheat. But also, care must be used in interpreting a graph such as Figure A1 where fluidity curves have been normalized about one point, in this case the point where $L_f \text{ rel} = 1$.

This type of approach, use of velocity times time in the fluid state, is subject to criticism. Firstly, an average velocity, usually equal to half the maximum velocity, was used as an approximation. It has been shown that under certain conditions the velocity gradually decreases and most of the flow occurs during the time of maximum velocity. But under other conditions there is negligible decrease of velocity until a sudden cessation occurs. In either case using an average velocity of half the maximum is a poor approximation. The velocity is determined by pressure applied and hydraulic resistances to flow. None of the analyses above have considered these factors. Secondly, a constant heat flow rate was assumed. In fact, the heat flow was not constant but varied with time. This effect can be large as will be shown.

The second approach to the mechanism governing fluidity has been from the fluid flow standpoint. In 1938 Lips and Nipper²⁷ investigated the viscosities of melts with various amounts, shapes, and sizes of solid particles. For a certain size and shape particle there existed a "critical" concentration of solid which caused an inordinate increase in viscosity. This critical concentration was lower for smaller particles and for more complicated shapes. These investigators also followed the freezing procedure of flowing solutions of potassium nitrate in water. (It is interesting that with an equilibrium solid concentration of only 14% the water solution became mushy and stopped flowing.) The solid was a white precipitate and could be easily observed. Streams of varying concentration of KNO_3 flowed identically as long as no precipitate was seen. The precipitate originated near the tip of the stream and was always

densest at that point. The authors concluded that flow was divided into two sections; the first section had no solid and flow was determined only by viscosity against the mold wall; the second section had solid particles and flow was predominantly determined by internal friction due to these particles. Flow ceased when the critical concentration was reached - this concentration depended on size and shape of the solid particles. This analysis seems quite advanced for the time, 1938; however, it is based on the assumption that solid particles form and flow in the liquid. As yet this assumption has not been proven for solidifying metals.

The first real analysis was made by Ruff in 1936⁴⁵. He measured velocities and determined friction factors under various conditions. He concluded that the flow of steel and cast iron resembled that of an ordinary turbulent liquid. He assumed that a stationary wall of liquid and solid existed next to the mold. Assuming steady state heat flow, he derived:

$$V_w = \frac{8 (T_s - T_k) \epsilon}{\rho C (T_i - T_s)} \frac{1}{4 r^2 \ln \frac{R}{r}} \quad (A5)$$

where V_w = velocity in the direction of flow of turbulent
molten particles next to the stationary wall

T_s = temperature in stationary zone

T_k = mold wall temperature

ϵ = thermal conductivity of metal in stationary zone

Varying the parameters $T_s - T_k$, $T_i - T_s$, R and ϵ , Ruff plotted the thickness of the stationary zone, $\delta = R - r$, versus V_w . This graph, Figure A2, shows that as δ increases above 0.2 mm, the velocity decreases rapidly. Ruff assigned $\delta = .2\text{mm}$ as the end point of flow.

In 1946 Rabinovich⁴¹ reviewed Ruff's assumptions and found his results as concerns friction factors to be in error. Unfortunately,

Rabinovich's equation for friction factors is not correct. However, he did measure velocity distribution in flowing metals and found metals to exhibit properties typical of liquids.

In 1953 Rightmire and Taylor⁴⁴ published an authoritative analysis of the flow and solidification of iron and steel. Ruff's data for iron and steel was analyzed and found to correspond to turbulent fluid flow in rough pipes as far as friction factors were concerned. By assuming steady heat flow the following equation was derived for fluidity at "high" superheat:

$$\frac{fL_f}{D} = \left[\frac{3fpc V_i}{8\gamma} \ln \frac{T'}{1 + \frac{\gamma}{\beta}} + 1 \right]^{\frac{2}{3}} - 1 + \frac{7fpc V_i}{384 \gamma} \frac{\gamma D}{k} \left[\frac{3fpc V_i}{8\gamma} \ln \frac{T'}{1 + \frac{\gamma}{\beta}} + 1 \right]^{-\frac{1}{3}} \quad (A6)$$

where γ = coefficient of heat transfer from surface of
fluid to mold

β = coefficient of heat transfer for the fluid stream

k = thermal conductivity of the non-fluid metal.

The heat of fusion does not appear in this equation because the theory provides that the flow stops before any appreciable quantity of solid forms. The frictional force which impedes and eventually stops the flow occurs at the boundary between the flowing core and non-flowing wall of metal, the latter being almost all liquid. The logarithmic terms of equation (A6) go to zero and negative values when the relative superheat, T' , equals $(1 + \gamma/\beta)$ or drops below $(1 + \gamma/\beta)$. Thus equation (A6) holds only when $T' > (1 + \gamma/\beta)$. Since Rightmire and Taylor report expected values of $(1 + \gamma/\beta)$ to be 1.01 to 1.02 for steel, a new analysis for low superheat was needed. They assumed that flow ceases due only to the increase in viscosity which was said to increase logarithmically as the temperature decreased to the melting point. Equation (A7) was then derived for the case of low superheat.

$$\frac{fL_f}{D} = R \frac{fpc V_i}{8\gamma} \left(1 - \frac{1}{T'} \right) \quad (A7)$$

Equations (A6) and (A7) were very advanced at the time although they are quite applicable today. The following limitations should be mentioned: 1) The analysis was made for, and checked by data from, steel fluidity tests by various investigators using widely varying conditions. Its applicability to other alloys has not been attempted or checked. 2) The heat flow was assumed to be steady, that is independent of time. After Adam's¹ analysis of freezing in molds it is well known that heat flow rate decreases with time. 3) The analysis for low¹ superheat is questionable due to the assumed behavior of the viscosity with temperature. Fisher and Phillips¹⁴ have shown that viscosities of Sn, Sb, Cd, and Pb do not increase in the manner assumed.

In 1953 Ragone et al.⁴² conducted an analysis of fluidity of pure metals. By assuming 1) that a solid ring freezes off and stops the flow, and 2) that heat flow was independent of time, they developed equation (A8) for fluidity at the melting point:

$$L_f = \frac{V_i R}{2h} \frac{PH}{T_m - T_r} F\left(\frac{V_i f}{2h} \frac{PH}{T_m - T_r}\right) \quad (A8)$$

where $F(x)$ is a modifying function resulting from the application of Simpson's Rule to solve numerically differential equation (A9).

$$V_e^2 = \left(\frac{dL_e}{d\theta}\right)^2 = \frac{V_i^2}{1 + \frac{f}{8r_i^4} \left(\frac{R^4 - r_i^4}{R - r_i}\right) L_e} \quad (A9)$$

where r_i = liquid metal radius at $L = 0$.

With superheat, Ragone et al. assumed, as did most others, that an initial length, L_1 , was provided by the metal losing heat till the melting

temperature was reached. Then fluidity proceeded according to equation (A8) using the velocity, V_1 , of the stream at the time the melting temperature was reached.

$$V_1 = \frac{V_i}{\sqrt{1 + f \frac{L_1}{2R}}} \quad (\text{A10})$$

L_1 was determined using the same analysis as Rightmire and Taylor:

$$L_1 = \frac{2R}{f} \left[\left\{ \frac{3}{8} \frac{f \rho c V_i}{h} \ln T' + 1 \right\}^{2/3} - 1 \right] \quad (\text{A11})$$

Equation (A11) is identical with the first half of equation (A6). Once L_1 was known, V_1 could be found using (A10). Then L_f was the sum of L_1 and L_2 :

$$L_f = L_1 + \frac{V_1 R}{2h} \frac{\rho H}{T_m - T_r} F \left(\frac{V_1 f}{2h} \frac{\rho H}{T_m - T_r} \right) \quad (\text{A12})$$

Ragone et al. applied Adam's equation¹ for time-dependent heat flow in molds such as sand. Using this condition he derived equation (A13) for a pure metal at its melting point.

$$L_f = \frac{V_i R^2 \pi}{k' \rho' c'} \left[\frac{\rho H}{T_m - T_r} \right]^2 G \left(\frac{f V_i R \pi}{k' \rho' c'} \left[\frac{\rho H}{T_m - T_r} \right]^2 \right) \quad (\text{A13})$$

where $G(x)$ is a modifying function resulting from the application of Simpson's Rule to solve numerically differential equation (A14):

$$V_e^2 = \left(\frac{dL_e}{d\theta} \right)^2 = \frac{V_i^2}{1 + \frac{f}{8r_i^4} \left(\frac{R^4 - r_i^4}{R - r_i} \right) \frac{V_i}{2\theta_f} (\theta_f^2 - [\theta_f - \theta]^2)} \quad (\text{A14})$$

Unfortunately two approximations used in equation (A14) were derived and validated for the case in which heat flow was assumed independent of time. These approximations were 1) that the liquid-solid interface was conical in shape, and 2) that stream velocity decreased linearly with time. The present work will show that these approximations are not valid for the case of time dependent heat flow.

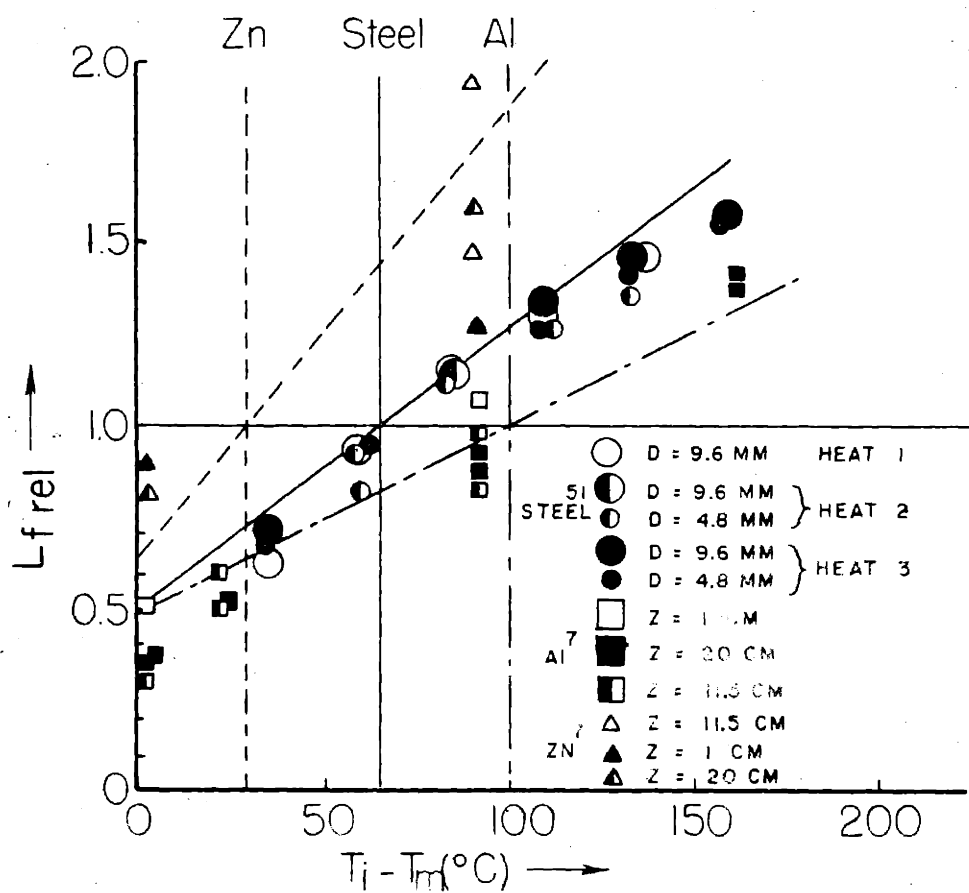


FIG. A1 KLYACHKO AND KUNIN GRAPH OF RELATIVE FLUIDITY

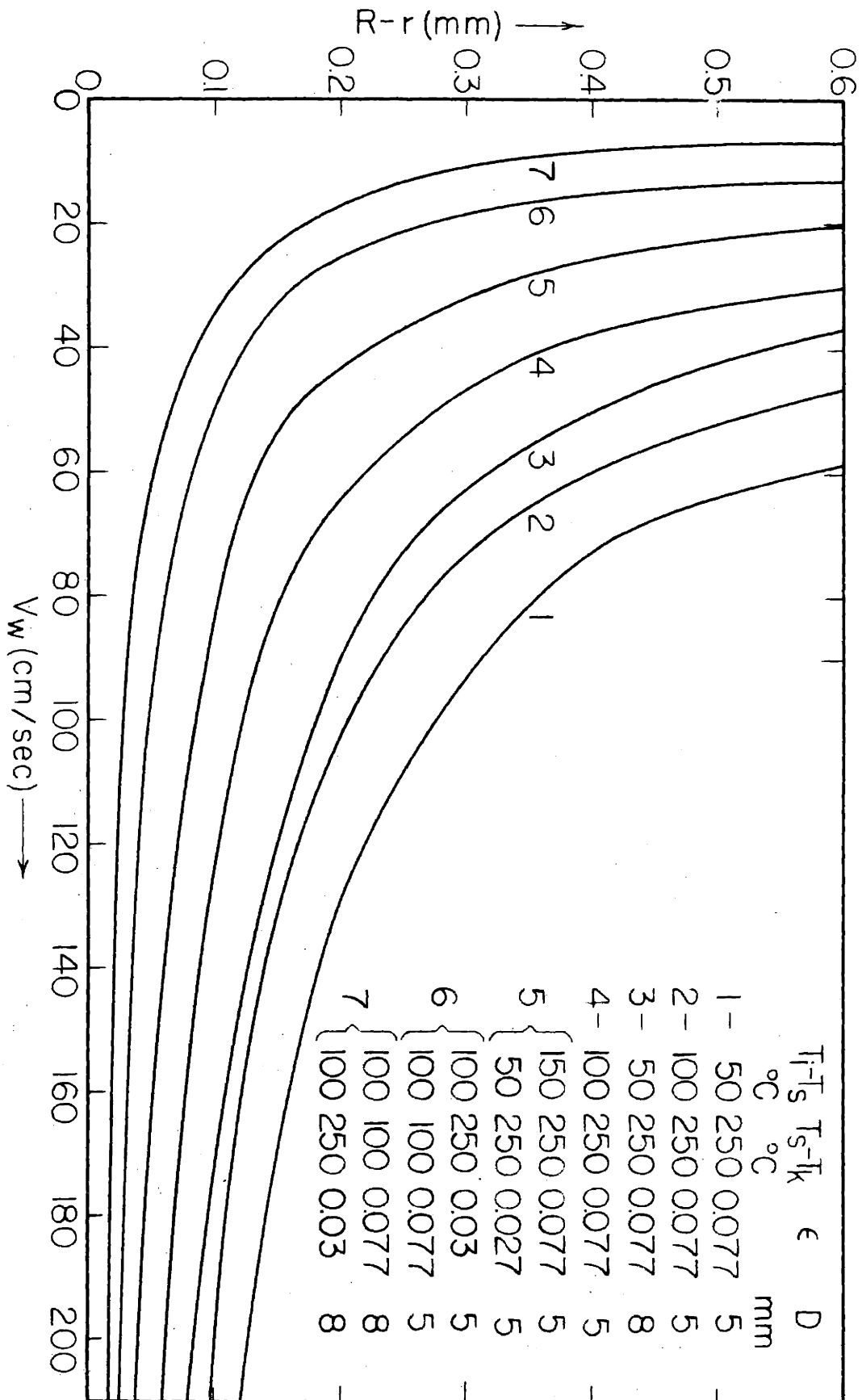


FIG. A2 RUFF'S GRAPH OF STATIONARY WALL THICKNESS AS A FUNCTION OF METAL VELOCITY AT THE WALL

APPENDIX B

DETERMINING ENERGY LOST FROM SOLID METAL BEFORE
FLOW CEASES FOR A PURE METAL

Figure B1 shows an expanded cross section of the fluidity stream at the instant flow ceases. At the completely solid cross section the solid metal will have lost more energy than at any other cross section. This analysis is for a volume of unit length at the solid cross section.

From Adams¹ for solidifying cylinders at the instant of final freezing:

$$\frac{Q_C}{Q_H} = \frac{R^2}{4 \alpha \theta_f}$$

where Q_C = heat lost from solid metal

Q_H = heat of fusion of solid metal.

Figure B2 shows Q_C/Q_H as a function of θ_f for pure tin in the two sizes of tubes used in this work. Since only the small size was used for pure metals, it can be seen that Q_C is only 2% of Q_H if the freezing time is close to 1.5 sec. In the experimental section of this paper all freezing times for pure tin were above 1.4 secs.

Equation (B1) shows that metals with a high heat diffusivity lose very little heat from the solid prior to the cessation of flow. Since tin has a low heat diffusivity relative to other pure metals, it follows that other metals will lose less energy from the solid prior to completion of a fluidity run.

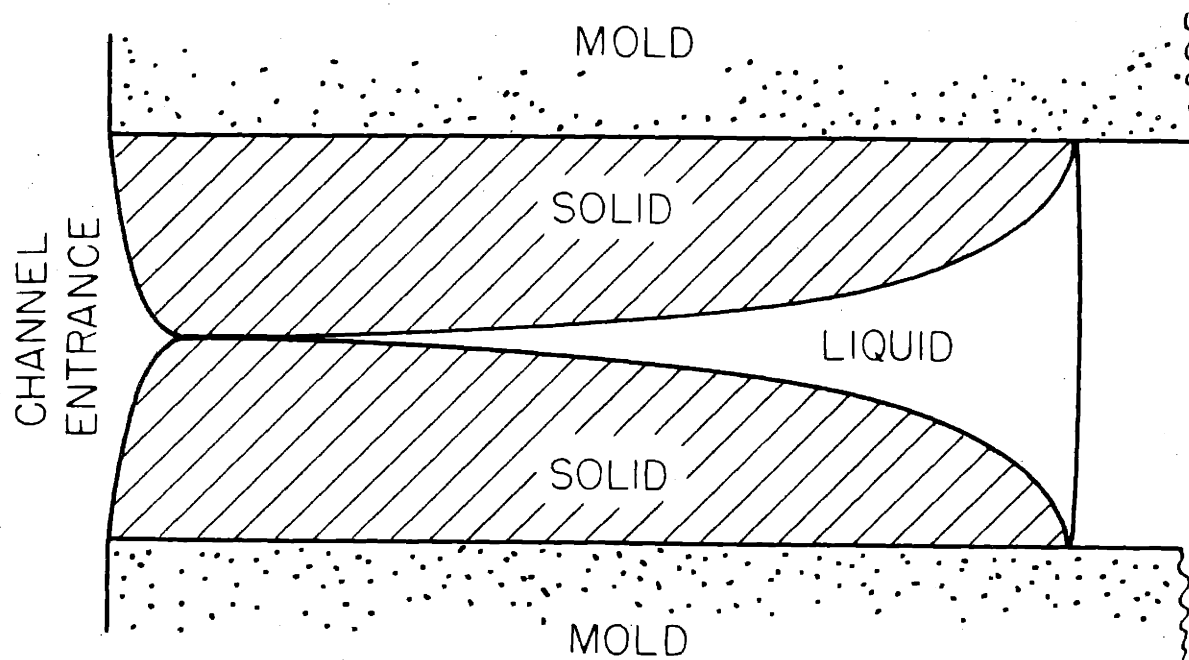


FIG. B1 SCHEMATIC CROSS SECTION OF FLUIDITY STREAM
AT THE TIME FLOW CEASES

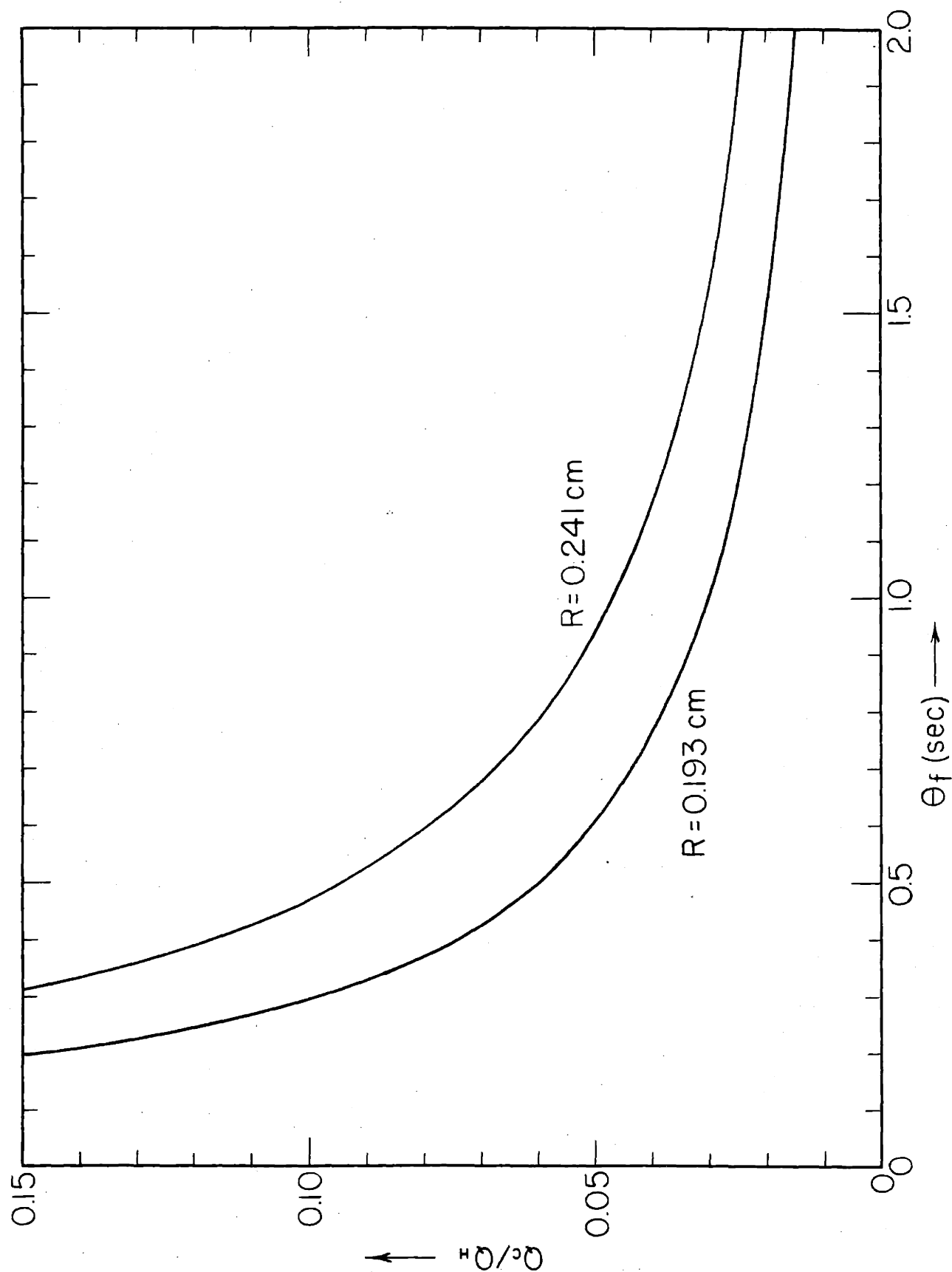


FIG. B2 ENERGY FROM SOLID METAL AS A FUNCTION OF FREEZING TIME AND TUBE RADIUS

APPENDIX C

EVALUATION OF FRICTION FACTOR

The Reynolds number, N_{Re} , may be easily evaluated for the portion of the mold channel where there is no freezing on the wall of the channel.

$$N_{Re} = \frac{2 R V_e \rho}{\mu} \quad (C1)$$

When a layer of stationary metal is adjacent to the mold wall, the radius of flow is reduced. Equation (C1) for any cross-section becomes:

$$N_{Re} = \frac{2 r V \rho}{\mu} \quad (C2)$$

Conservation of matter requires that:

$$\pi r^2 V = \pi R^2 V_e$$

or:

$$V = \frac{R^2}{r^2} V_e \quad (C3)$$

Substituting (C3) in (C2) yields:

$$N_{Re} = \frac{R}{r} \frac{2 R V_e \rho}{\mu} \quad (C4)$$

Since R/r is always greater than one, it follows that the minimum Reynolds number results when r is a maximum or when r equals R ; then equation (C4) reduced to (C1).

Figure C1 shows values of N_{Re} from equation (C1) at the start of fluidity tests for typical values of R as a function of V_i . Note that V_i equals V_e at the start of a fluidity test. According to experience in turbulent flow, once turbulence is established a transition period is necessary to eliminate it even though conditions are favorable for laminar flow. It is generally considered that a Reynolds number below 2,100 always results in laminar flow. Figure C1 shows that initial velocities of over 100 cm/sec always result in turbulent flow. Ideally this velocity corresponds to a metal head of 3.26 cm, but in practice it is somewhat larger due to energy losses in the initial flow. Even so, metal heads of 5 cm (about 2 inches) are much smaller than common practice. Figure C1 shows Reynolds number for tin in the small tubes used in this research. The flow may be considered only as turbulent.

The friction factor for turbulent flow depends on the surface roughness and, to a much lesser extent, the Reynolds number. Figure C2 shows the relation between friction factor and Reynolds number. For friction factor of 0.04 and above, there is practically no variation in friction factor.

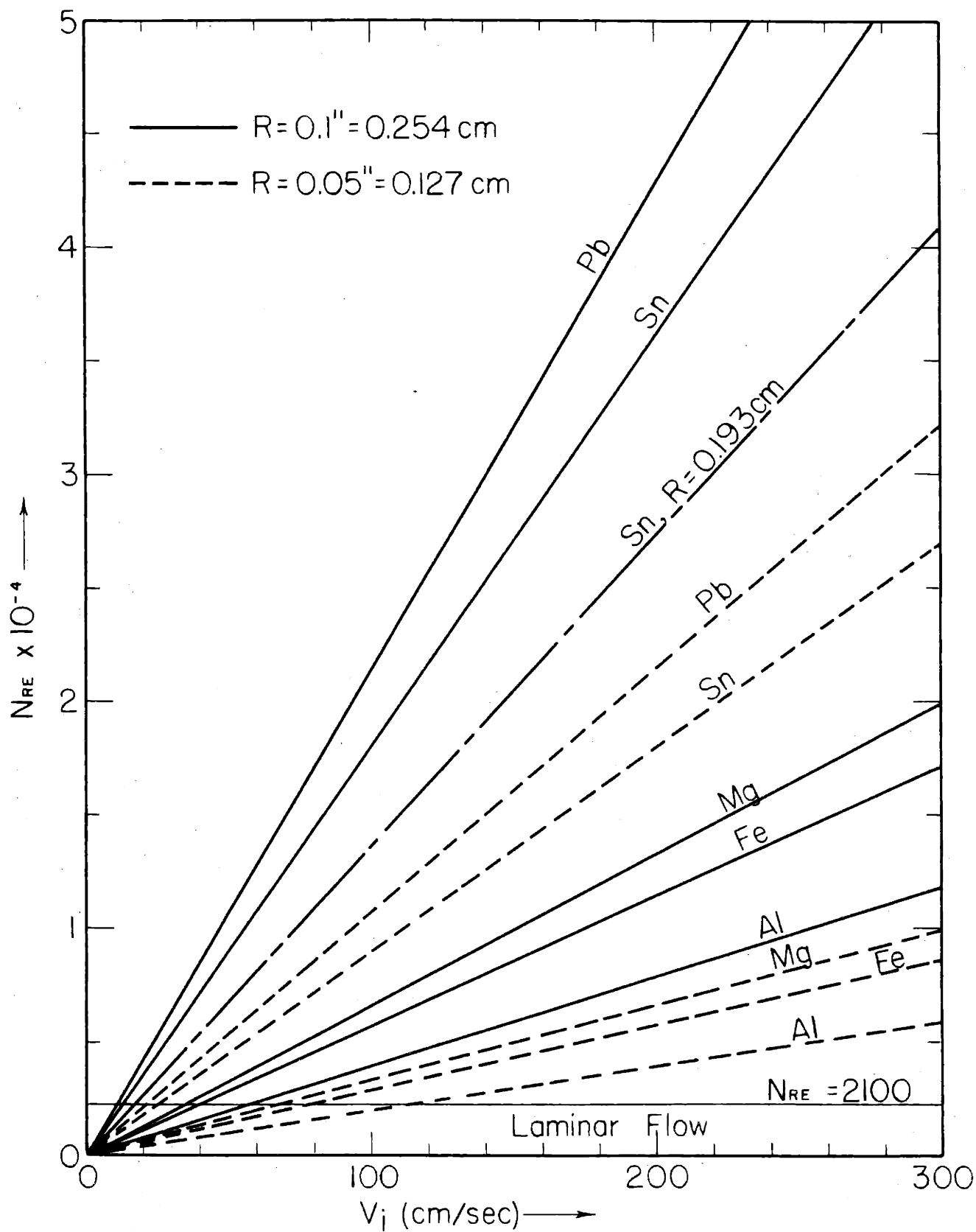


FIG. C1 REYNOLDS NUMBER FOR FLUIDITY TESTS FROM EQUATION (C1)

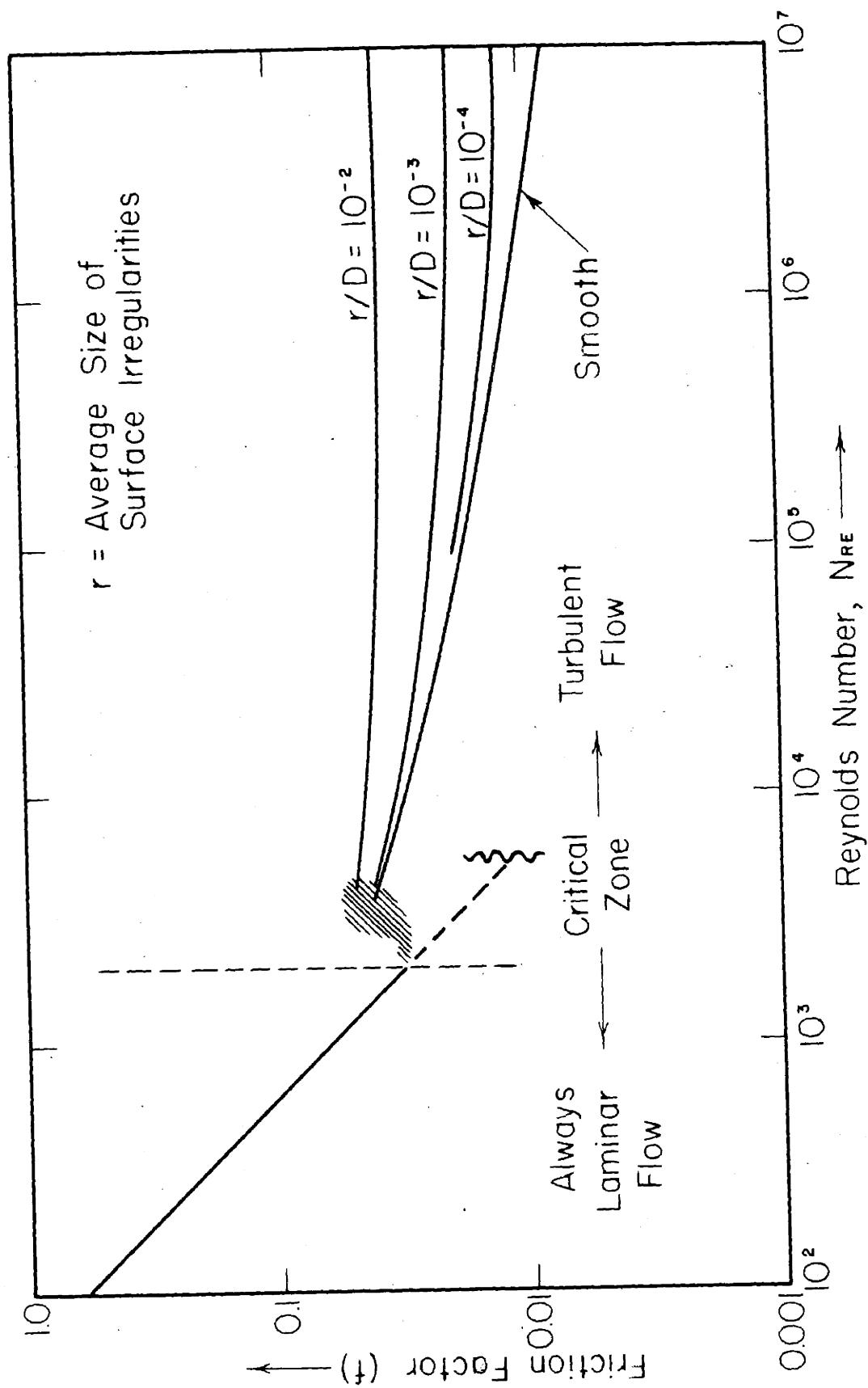


FIG. C2 FRICTION FACTOR VERSUS REYNOLDS NUMBER IN LONG, STRAIGHT DUCTS
(AFTER MOODY, REF. 32)

APPENDIX D

HEAT FLOW IN CYLINDRICAL CHANNELS

Figure D1 shows temperature distribution according to the assumption that resistance to heat flow arises only at the metal-mold interface and in the mold itself. At the interface the rate of heat flow per unit length of cylinder from the metal is:

$$q = 2\pi R h (T - T_{sc}) \quad (D1)$$

Using Adams's equation¹ the heat flow rate per unit length into an "infinite" cylindrical mold is:

$$q = 2\pi R (T_{sc} - T_r) k' \left[\frac{1}{2R} + \frac{1}{\sqrt{\pi \alpha'} \sqrt{\theta_h}} \right] \quad (D2)$$

Rearranging so that the temperature terms alone are on the same sides of (D1) and (D2) and then adding yields:

$$(T - T_r) = (T - T_{sc}) + (T_{sc} - T_r) = q \left[\frac{1}{2\pi R h} + \frac{1}{2\pi R k' \left[\frac{1}{2R} + \frac{1}{\sqrt{\pi \alpha'} \sqrt{\theta_h}} \right]} \right] \quad (D3)$$

Combining and using $\alpha' = \frac{k'}{\rho' c'}$ gives:

$$q \equiv \frac{dQ}{d\theta} = 2\pi R h (T - T_r) \left[\frac{\sqrt{\theta_h}}{\left(1 + \frac{2Rh}{k'}\right) \sqrt{\theta_h} + \frac{2R}{\sqrt{\pi \alpha'}}} + \frac{\frac{2R}{\sqrt{\pi \alpha'}}}{\left(1 + \frac{2Rh}{k'}\right) \sqrt{\theta_h} + \frac{2R}{\sqrt{\pi \alpha'}}} \right] \quad (D4)$$

(D4) is a differential equation in terms of Q and θ_h . The variables are separable and the equation may be integrated by simple substitutions.

For simplification let

$$\left. \begin{aligned} A &\equiv \frac{2R}{\sqrt{\pi\alpha'}} \sec^{\frac{1}{2}} \\ B &\equiv \left(1 + \frac{2Rh}{k'}\right) \end{aligned} \right\} \quad (D5)$$

Then (D4) reduces to:

$$dQ = 2\pi Rh(T - T_r) \left[\frac{\sqrt{\theta_h}}{B\sqrt{\theta_h} + A} + \frac{A}{B\sqrt{\theta_h} + A} \right] d\theta \quad (D6)$$

Integration between the limits 0 to Q and 0 to θ_h yields:

$$Q = \frac{2\pi Rh(T - T_r)}{B} \left[\theta_h + 2A\left(1 - \frac{1}{B}\right)\sqrt{\theta_h} - \frac{2A^2}{B}\left(1 - \frac{1}{B}\right)\ln\left(1 + \frac{B}{A}\sqrt{\theta_h}\right) \right] \quad (1), (D7)$$

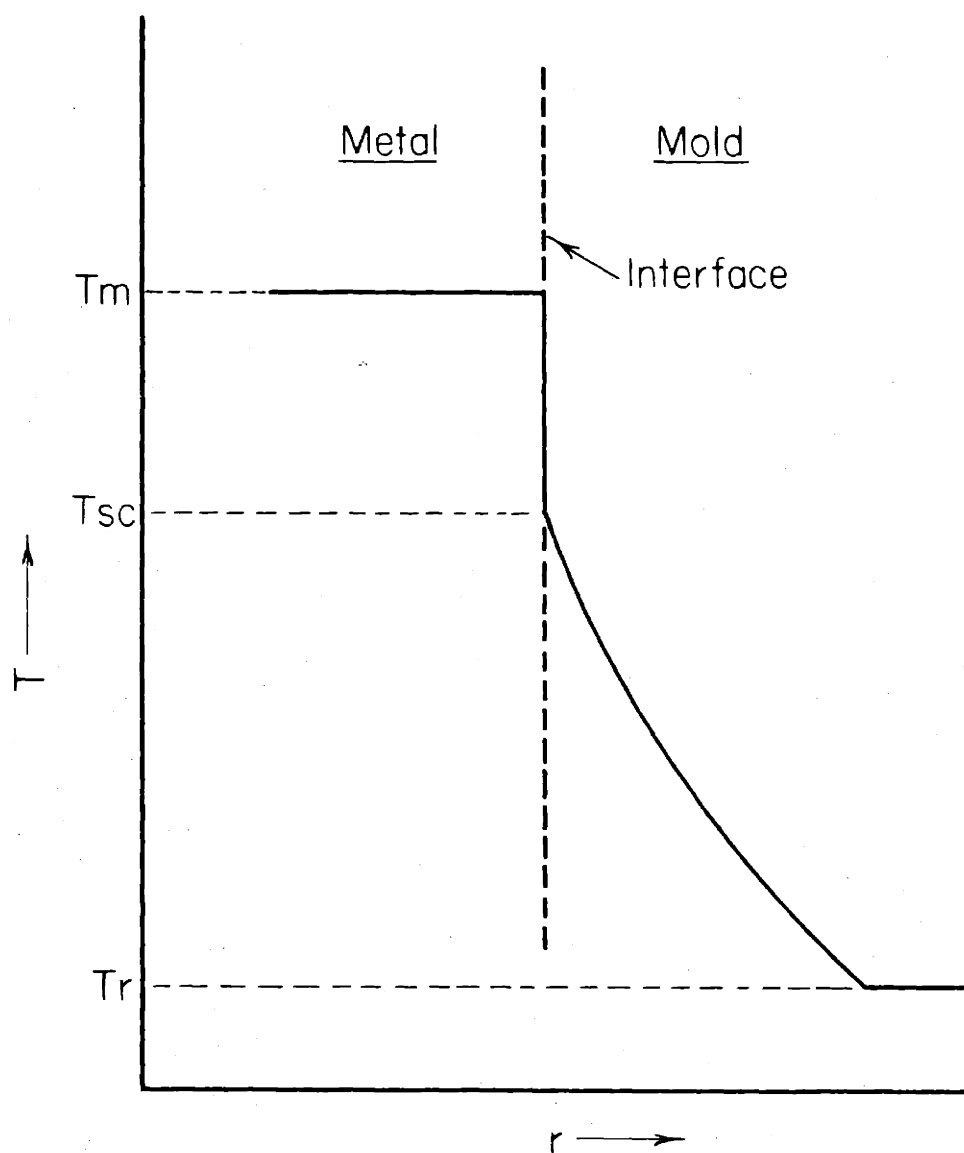


FIG. D1 SCHEMATIC TEMPERATURE DISTRIBUTION IN METAL AND MOLD

APPENDIX E

FACTORS AFFECTING VELOCITY

If 1) acceleration effects are neglected, 2) the pressure at the end of the metal stream is constant, 3) energy losses occur only in "entrance loss" and wall frictional losses, and 4) solid (or stationary liquid) forms only at mold walls, then the flow can be related by Bernoulli's equation for an energy balance:

$$Z_1 + \frac{V_1^2}{2g} + \frac{P_1}{\rho} = Z_e + \frac{V_e^2}{2g} + \frac{P_e}{\rho} + \phi_{ent} \frac{V_e^2}{2g} + \int_0^{L_e} \frac{f V^2}{2g} \frac{dL}{2r}$$

or:

$$2g \left(Z_1 - Z_e + \frac{P_1 - P_e}{\rho} \right) = V_e^2 (1 + \phi_{ent}) + \int_0^{L_e} \frac{f V^2}{2r} dL \quad (E1)$$

where P = pressure

$Z_{()}$ is height above a datum

1 refers to pouring end of liquid metal system

e refers to the end of the metal stream.

Let $Z \equiv \left(Z_1 - Z_e + \frac{P_1 - P_e}{\rho} \right) \quad (E2)$

Conservation of matter requires that volume flow rate be constant at every point in the mold for a particular time. Then, since the end of the stream has no solid:

$$\pi r^2 V = \pi R^2 V_e$$

or

$$V = \frac{R^2}{r^2} V_e \quad (E3)$$

Substituting (E2) and (E3) in (E1) and rearranging yields:

$$V_e = \frac{\sqrt{2gZ}}{\sqrt{1 + \phi_{ent}}} \frac{1}{\sqrt{1 + \frac{fR^4}{2(1+\phi_{ent})} \int_0^{L_e} \frac{dL}{r^5}}} \quad (E4)$$

At the start of the flow L_e equals zero (i.e., there is no wall frictional loss) and V_e equals V_i , and (E4) reduces to:

$$V_i = \sqrt{\frac{2gZ}{1 + \phi_{ent}}} \quad (E5)$$

Substituting (E5) in (E4) gives:

$$\frac{dL_e}{d\theta} = V_e = \frac{V_i}{\sqrt{1 + \frac{fR^4}{2(1+\phi_{ent})} \int_0^{L_e} \frac{dL}{r^5}}} \quad (2), (E6)$$

APPENDIX F

EVALUATING SHAPE OF SOLID-LIQUID INTERFACE
FOR PURE TIN

In order to determine the shape of the solid-liquid interface one must solve equation (2) which can be solved numerically by an iterative process. r may be found as a function of time by use of equation (1) and equation (F1) which relates the energy removed to the heat of fusion for the amount of solid metal formed per unit length:

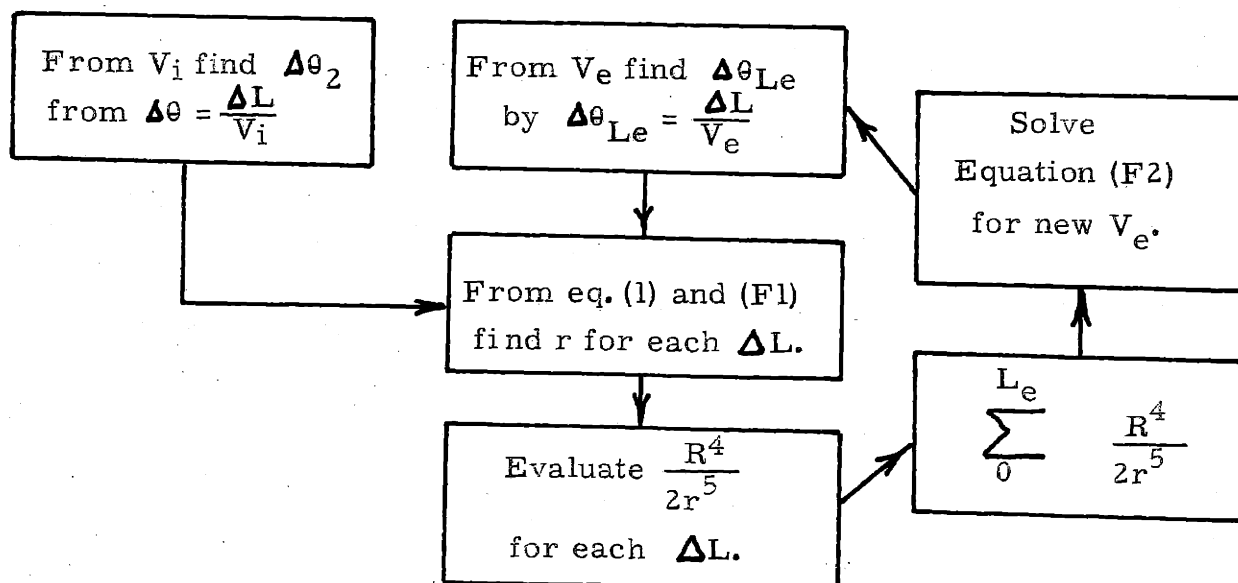
$$Q = \rho H \pi (R^2 - r^2) \quad (\text{F1})$$

For solving equation (2) numerically, it is modified to:

$$V_e = \frac{V_i}{\sqrt{1 + \frac{f \Delta L}{(1 + \phi_{ent})} \sum_{L=0}^{L_e} \frac{R^4}{2r^5}}} \quad (\text{F2})$$

where ΔL is the constant control interval.

Schematically the iterative process is represented by flow diagram:



This loop process is continued until V_e is reduced to zero. The start of one solution using this iterative process is shown in Table I.

The results of solutions of equation (2) are shown in Figure F1 which shows the solid-liquid interface for various times for a medium velocity ($V_i = 180$ cm/sec) fluidity test for tin with no superheat, in Figure F2 which shows the same except that velocity is low ($V_i = 100$ cm/sec) and in Figure F3 which shows the variation of velocity for the conditions of Figure F1.

Analysis of Figures F1 and F3 showed that r was a parabolic function of L of the type

$$r = R - K\sqrt{L_e - L} \quad (5), (F3)$$

where K is a function of V_e . For instance, for the curves of Figure F1:

$$K = \sqrt{\frac{0.0045}{V_e - 4} - 0.00002} \quad (F4)$$

Unfortunately the parabolic relationship breaks down as the velocity approaches zero. For equation (F4), the relationship is indeterminate when V_e is 4 cm/sec. Equation (F3) is shown on Figure F1; and the coincidence with the analyzed curves is excellent till θ is at least 1.06 sec (or till V_e is about 15 cm/sec).

TABLE I
START OF SOLUTION OF EQUATION (2)
USING ITERATIVE PROCESS

Conditions:

$$\begin{array}{ll}
 R = 0.193 \text{ cm} & \rho' = 2.53 \text{ gm/cm}^3 \text{ (Pyrex)} \\
 h = 0.18 \text{ cal/cm}^2 \text{ }^\circ\text{C sec} & \rho_H = 106 \text{ cal/cm}^3 \text{ (Tin)} \\
 c' = 0.228 \text{ cal/gm}^\circ\text{C} & f = 0.04 \\
 k' = .00295 \text{ cal/cm}^2 \text{ sec }^\circ\text{C/cm} & \phi_{\text{ent}} = 0.95 \\
 V_i = 180 \text{ cm/sec} & \Delta L = 2 \text{ cm} \\
 F = \frac{R^4}{2r^5} & T - T_r = 207^\circ\text{C}
 \end{array}$$

L

θ		2	4	6	8	10		F	V_e
.0111	θ_h r F	.0111 .1917 2.7						2.7	168
.0119		.0230 .188 3.0	.0110 1.917 2.7					5.7	157.5
.0127		.0357 .1865 3.1	.0246 .188 3.0	.0127 .1917 2.7				8.8	148.5
.0135		.0492 .184 3.3	.0381 .186 3.15	.0262 .188 3.0	.0135 .1917 2.7			12.15	140
.0143		.0635 .182 3.5	.0524 .1836 3.3	.0405 .1855 3.15	.0278 .1875 3	.0143 .190 2.8		15.75	132

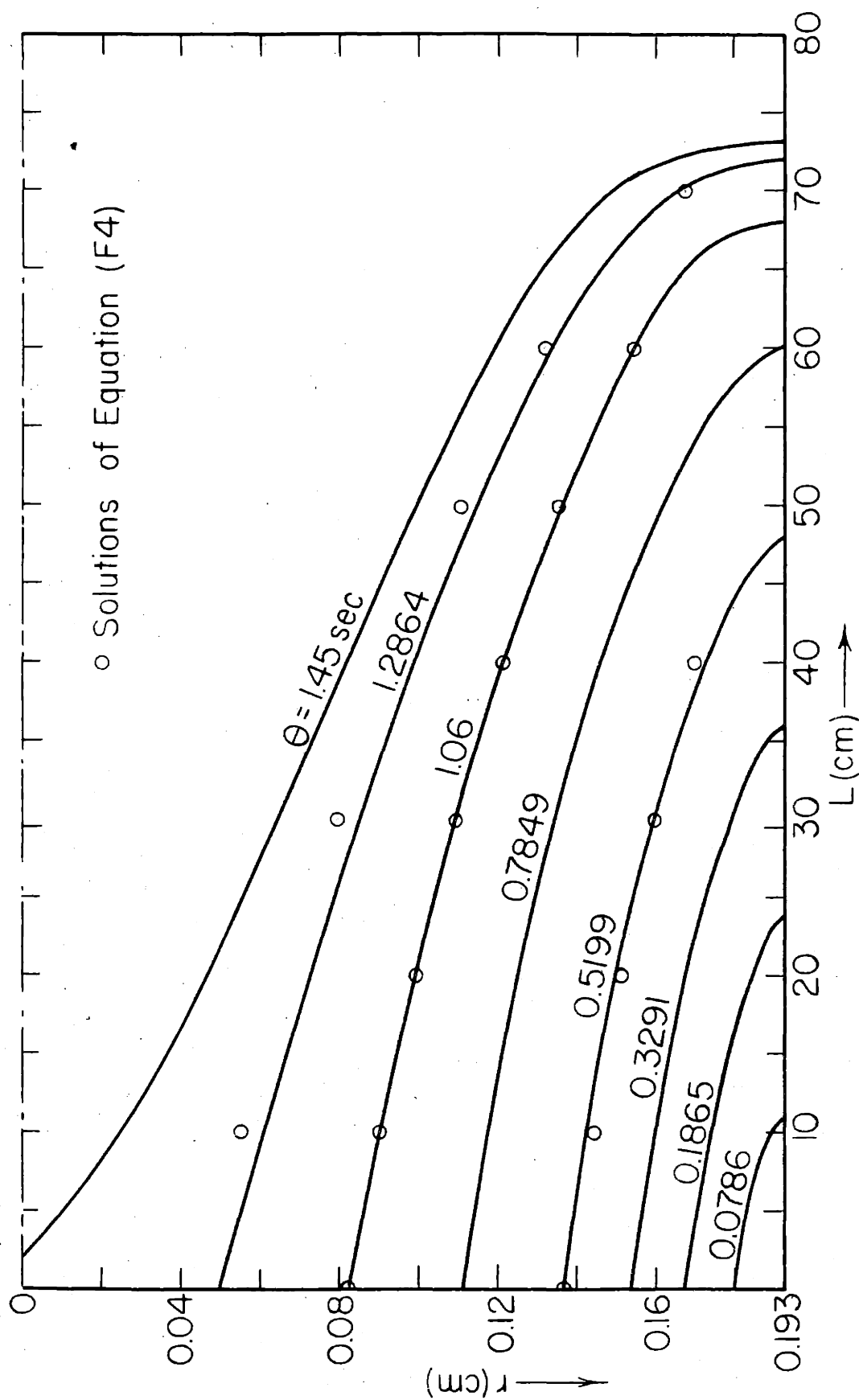


FIG. F1 SOLID-LIQUID INTERFACES FOR $V_i = 180 \text{ CM/SEC}$

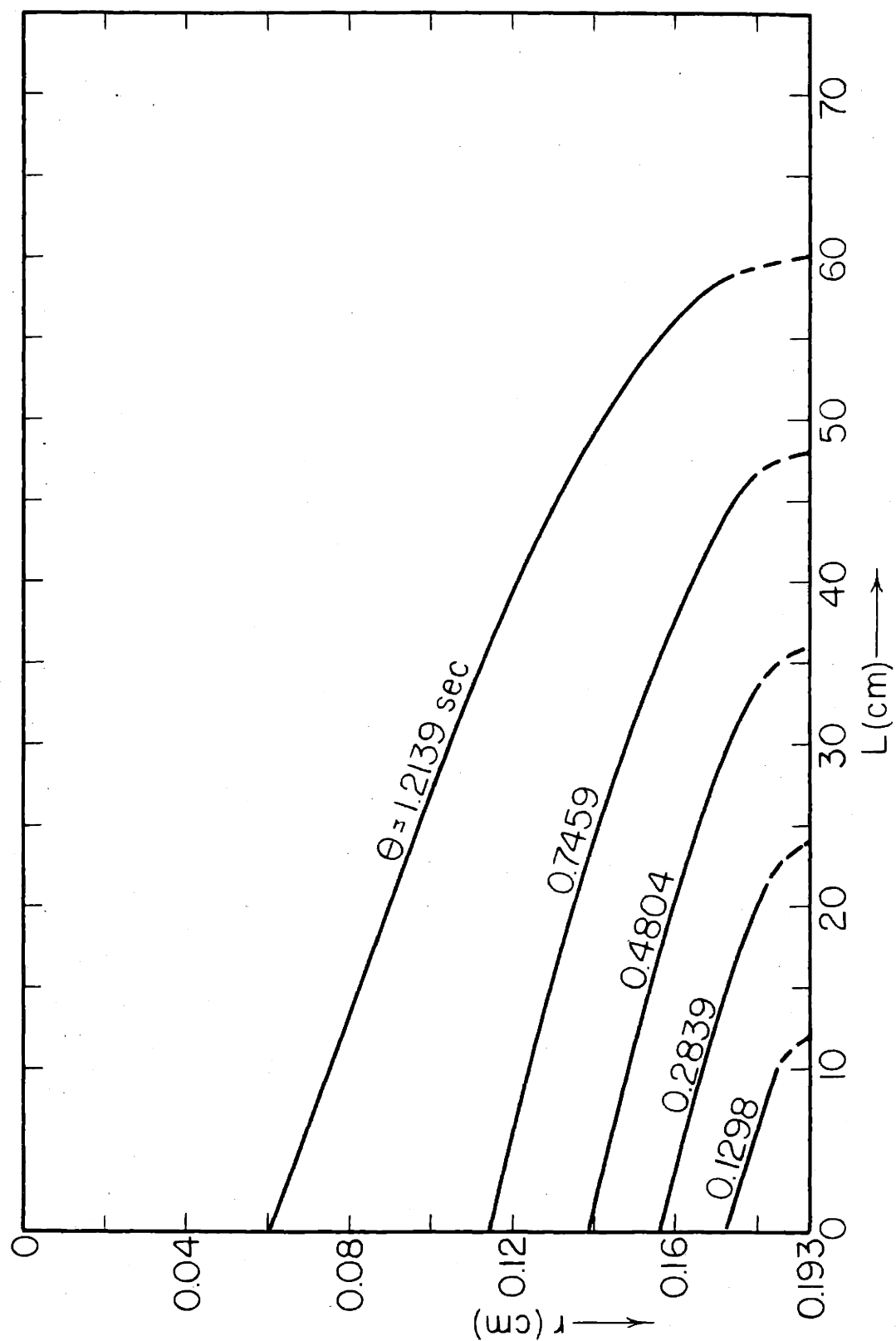


FIG. F2 SOLID-LIQUID INTERFACES FOR $V_i = 100$ CM/SEC

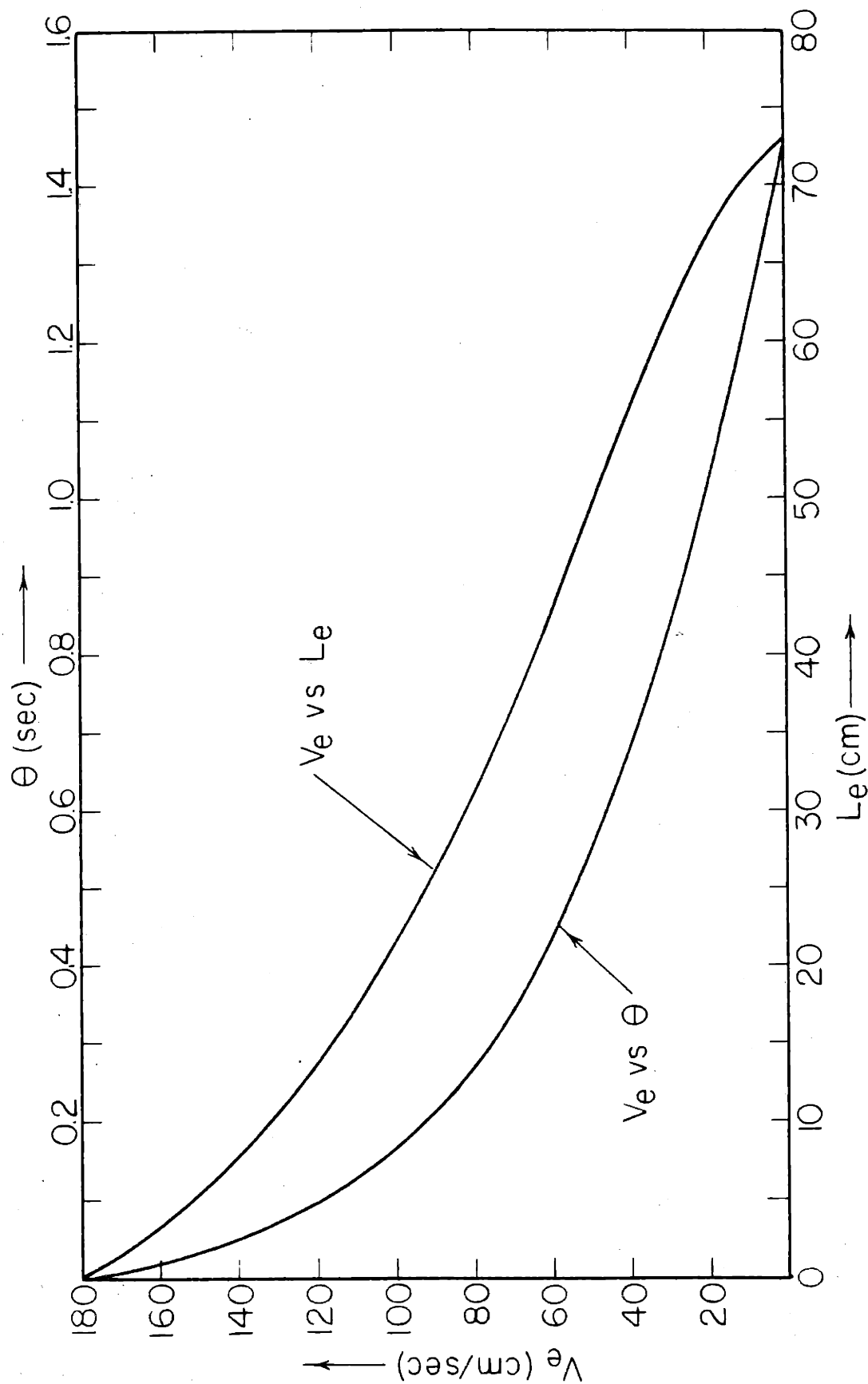


FIG. F3 STREAM VELOCITY AS A FUNCTION OF TIME, θ , AND LENGTH, L_e

APPENDIX G

CALCULATION OF MINIMUM INCREASE OF FLUIDITY DUE TO SUPERHEAT

Zone I is composed of entirely superheated metal so equation (4) governs the length as a function of time. If it is assumed that an element of liquid metal of length ΔL proceeds down the mold channel intact, then at successive intervals the decrease of temperature may be found by use of equations (1) and (9).

The procedure is: 1) find the time for the stream to flow ΔL , 2) determine the element of energy extracted from each ΔL for this time (note that θ_h is used for this calculation when equation (1) is used), 3) determine the decrease in temperature for each ΔL , and 4) advance the stream another ΔL and start with 1) again. This process is carried out in Table II. Note that $(T - T_r)$ is maintained constant and equal to $T_m - T_r$ in equation (1). If the initial metal temperature is not much above T_m , then equation (1) is accurate enough for these purposes. The maximum metal temperature in Table II is $T_m + 19.08^\circ\text{C}$. The metal stream has lost its superheat when $L_e = 5$ cm, and the value of $\frac{L_e}{T_i - T_m}$ is $0.227 \text{ cm}/^\circ\text{C}$.

TABLE II
CALCULATION OF DECREASE IN TEMPERATURE
FOR SUPERHEATED METAL

Conditions:

R	$= 0.193 \text{ cm}$	f	$= 0.04$
h	$= 0.18 \text{ cal/cm}^2 \text{ } ^\circ\text{C sec}$	ϕ_{ent}	$= 0.95$
c'	$= 0.228 \text{ cal/gm}^\circ\text{C}$	ΔL	$= 1 \text{ cm}$
ρ'	$= 2.53 \text{ gm/cm}^3$	ρ_c	$= 0.425 \text{ cal/cm}^3$
k'	$= 0.00295 \text{ cal/cm}^2 \text{ sec } ^\circ\text{C/cm}$	$T - T_r$	$= 207^\circ\text{C}$
V_i	$= 180 \text{ cm/sec}$	Q	$= \text{solution of equation (1)}$

		L(cm)				
$\theta(\text{sec})$		1	2	3	4	5
0.005	θ_h	0.005				
	Q	0.15				
	ΔQ	0.15				
	T	3.01				
0.01		0.015	0.005			
		0.4	0.15			
		0.25	0.15			
		5.02	6.02			
0.018		0.018	0.013	0.008		
		0.5	0.35	0.25		
		0.1	0.2	0.25		
		2.01	9.04	11.04		
0.025		0.025	0.02	0.015	0.007	
		0.63	0.53	0.4	0.2	
		0.13	0.18	0.15	0.2	
		2.61	5.62	12.05	15.06	
0.032		0.032	0.027	0.022	0.014	0.007
		0.75	0.7	0.6	0.4	0.2
		0.12	0.17	0.2	0.2	0.2
		2.41	6.02	9.64	16.07	19.08

APPENDIX H

LIMITS OF VALIDITY OF EQUATION (1)

To be valid, equation (D2), which is used to derive equation (1), must be applied only to molds which are "infinite"; that is, heat which leaves metal and enters the mold is inhibited only by the mold and is never able to leave the mold through any other interface. In these fluidity tests the tube wall is 0.092 cm thick for the smaller tubes - this thickness is "finite" if the outside wall temperature rises much above room temperature, because the outside wall is an interface which "reflects" energy back into the glass. Radiation and convection losses are considered nil.

To test validity, equation (D2) is compared to solutions of equations for materials of finite thickness. Unfortunately, the later solutions are not available for cylindrical tubes, so the comparison was made with plates and slabs. The equation analogous to (D2) for heat flow in an infinite plate is:

$$Q = AK(T_{sc} - T_r)2\sqrt{\theta_h} \quad (H1)$$

where A is the area considered.

If this heat is absorbed by a hypothetical slab of thickness t, the average temperature of the slab, T_{av} , is given by:

$$Q = \rho A t c (T_{av} - T_r) \quad (H2)$$

Equating (H1) and (H2) and rearranging gives:

$$\frac{T_{av} - T_r}{T_{sc} - T_r} = \frac{2\alpha' \sqrt{\theta_h}}{t} \quad (H3)$$

Hottel charts²⁹ applicable to finite slabs heated from both sides may be used to evaluate the heat into a slab wall heated on one side if the thickness of the latter is used instead of midplane distance of the former. The charts then give $(1 - \frac{T_{av} - T_r}{T_{sc} - T_r})$ as a function of $\frac{\alpha' \theta_h}{t^2}$.

In Figure H1 the data from the Hottel chart for the finite slab and equation (H3) for an infinite plate are plotted for two thicknesses as a function of time. It can be seen that up to 0.5 secs, equation (H3) accurately predicts heat flow; but above 0.5 secs equation (H3) indicates a greater rate of heat flow than the finite plate can handle.

The time at which this deviation introduces significant errors into equation (1) is somewhat longer than the time indicated on Figure H1. This is so because equation (1) is for cylindrical modls which show more "infiniteness" than flat plates of the same thickness and also involve an interface resistance to heat transfer. It is noted that equation (1) predicts a time of 2.1 secs for heat saturation of the smaller glass tube, equation (D2) predicts 1.39 secs and equation (H3) predicts 1.3 secs. An arbitrary limit to the deviation of the curves of Figure H1 is set at 15% difference, which should be considerably less than 10% for equation (1). The corresponding limits of time are about 1.5 secs for tubes of wall thickness 0.092 cm and 1.8 secs for thickness 0.1 cm.

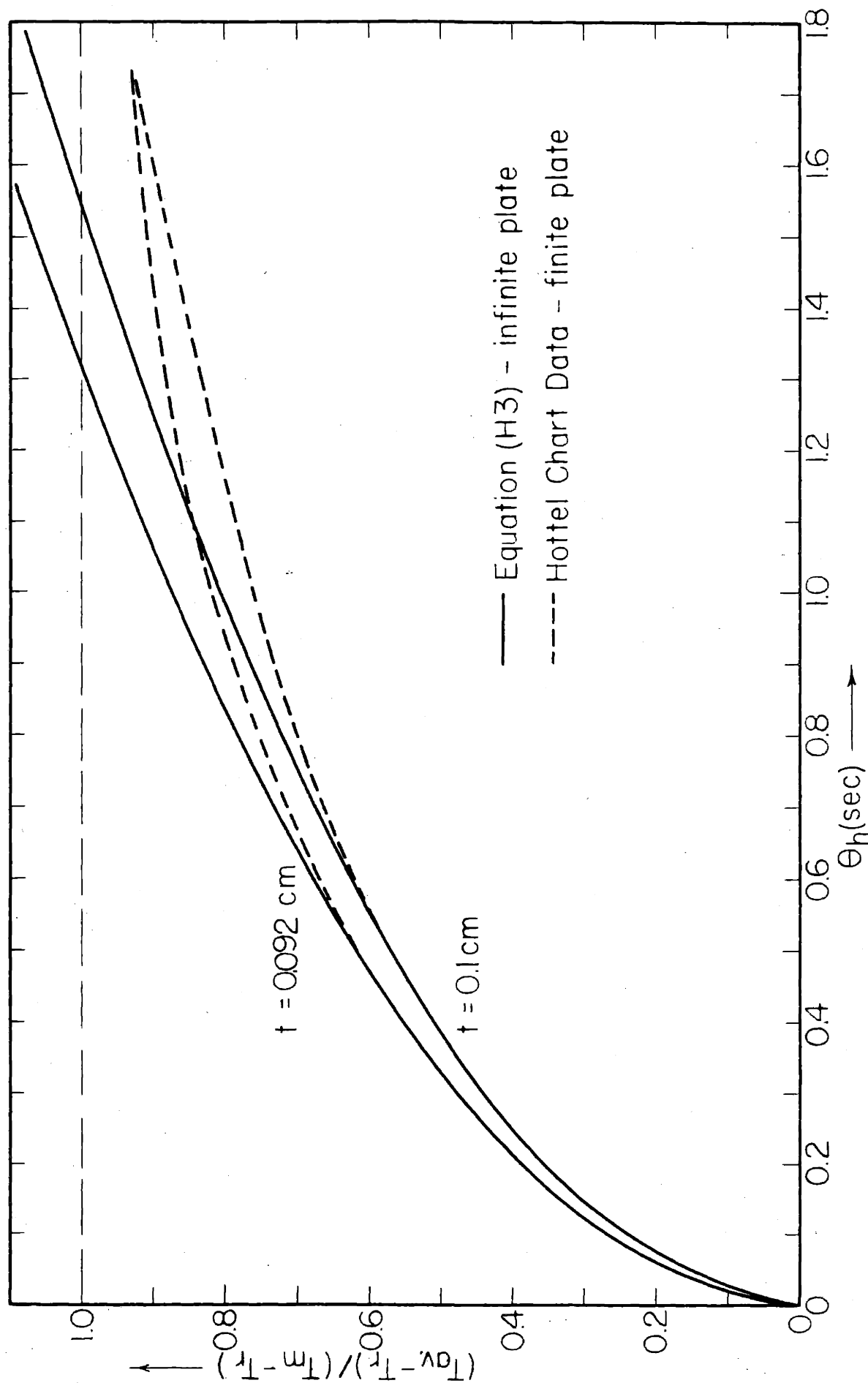


FIG. H1 HEAT ABSORPTION ABILITY OF INFINITE AND FINITE PLATES COMPARED

APPENDIX I

PHYSICAL PROPERTIES OF PYREX GLASS

The density of Pyrex changes negligibly with temperature; however, the heat content and thermal conductivity vary considerably as shown in Figure I1. It is almost imperative to use an effective average value for these two properties.

In order to determine suitable average values, an experiment was made measuring the freezing times for tin poured between thick Pyrex glass plates. The freezing times were measured with a thermocouple wired to a Sanborn recorder so that short times could be read. The result is Figure I2.

By using a similar analysis as in Appendix D, equation (II) for glass plate was derived:

$$Q = A(T_m - T_r) 2 \frac{K^2}{h} \left[\frac{h\sqrt{\theta_h}}{K} - \ln \left(\frac{h\sqrt{\theta_h}}{K} + 1 \right) \right] \quad (11)$$

where A is Area

$$K \equiv \sqrt{\frac{\rho'c'k'}{\pi}}$$

Also the heat lost by the freezing metal to each glass plate is:

$$Q = A \frac{\tau}{2} \rho H \quad (12)$$

where τ is the thickness of metal.

Equating (I1) and (I2) and simplifying:

$$\frac{\rho H}{4(T_m - T_r)} \frac{z}{K} = \sqrt{\theta_h} - \frac{\ln\left(\frac{h}{K}\sqrt{\theta_h} + 1\right)}{\frac{h}{K}} \quad (I3)$$

By using values of τ and θ from Figure I2, it soon becomes apparent that h is very large (over 10^5) for this experiment. The right side of equation (I3) reduces to $\sqrt{\theta_h}$ and (I3) reduces to:

$$K = \frac{\rho H}{4(T_m - T_r)} \frac{z}{\sqrt{\theta_h}} \quad (I4)$$

From this equation K was found to be 0.0235. The only temperature for which the properties of glass satisfy this value for K is 200°C where:

$$c' = 0.243 \text{ cal/gm}^\circ\text{C (average of two curves on Figure I1)}$$

$$k' = 0.00305 \text{ cal/gm sec}^\circ\text{C/cm}$$

It is reasonable that the effective values correspond to a temperature in the upper half of the range ($T_m - T_r$) since all of the heat must pass through the hottest part of the mold.

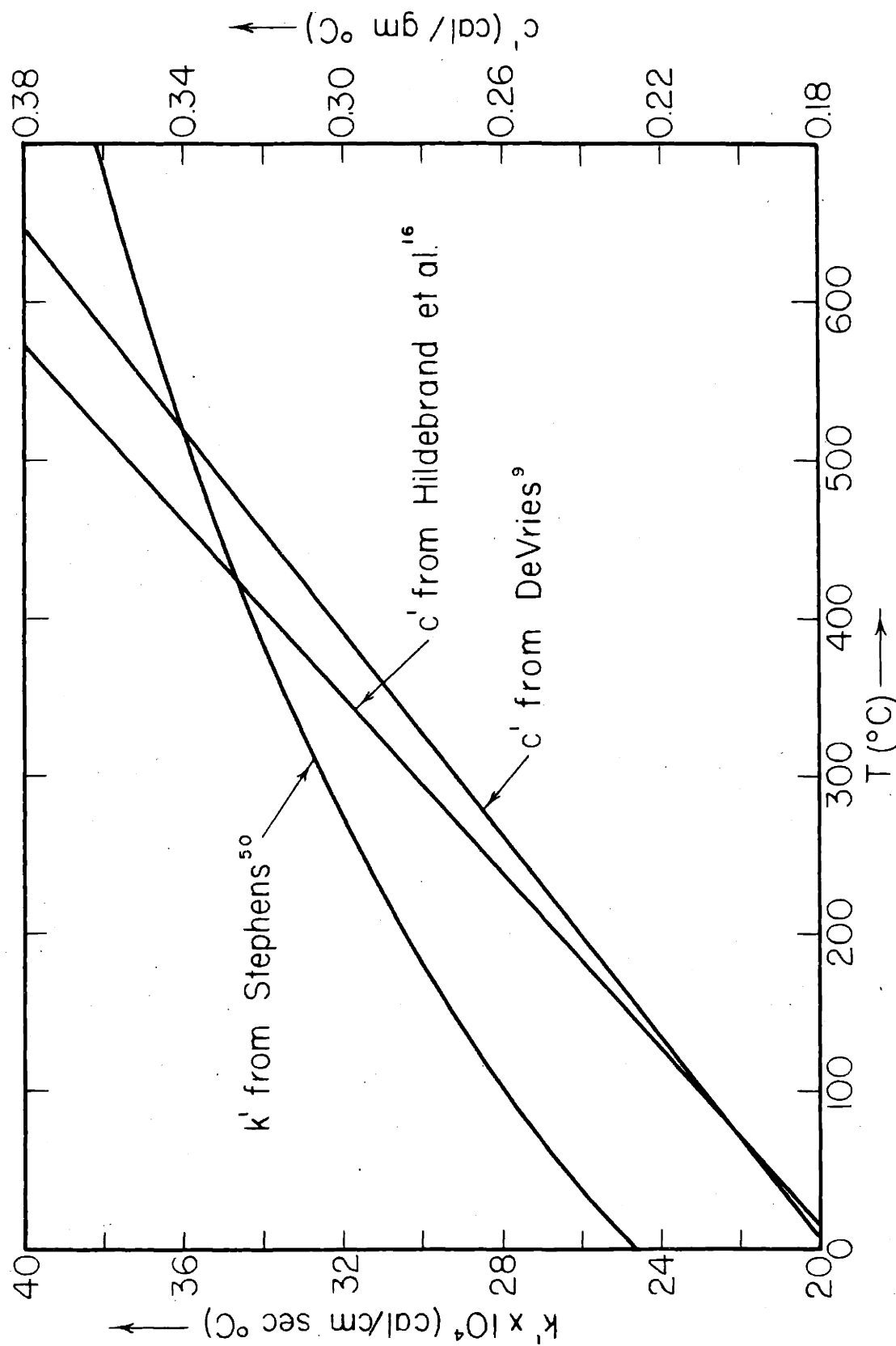


FIG. 11 HEAT CONTENT AND THERMAL CONDUCTIVITY OF PYREX GLASS AS FUNCTIONS OF TEMPERATURE

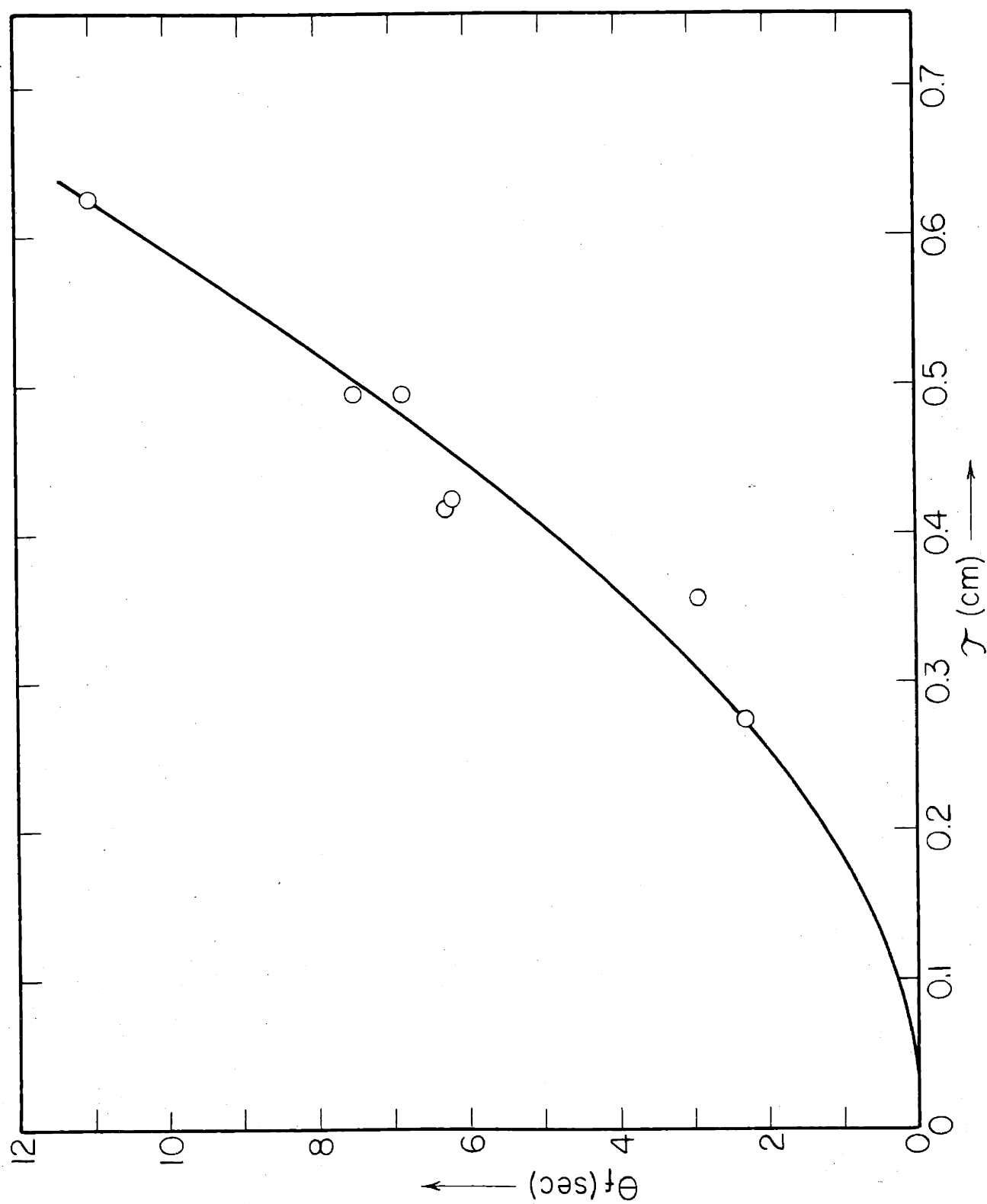


FIG.12 FREEZING TIME FOR TIN AS A FUNCTION OF DISTANCE BETWEEN PYREX PLATES

APPENDIX J

FLUIDITY AND FLUID LIFE DATA

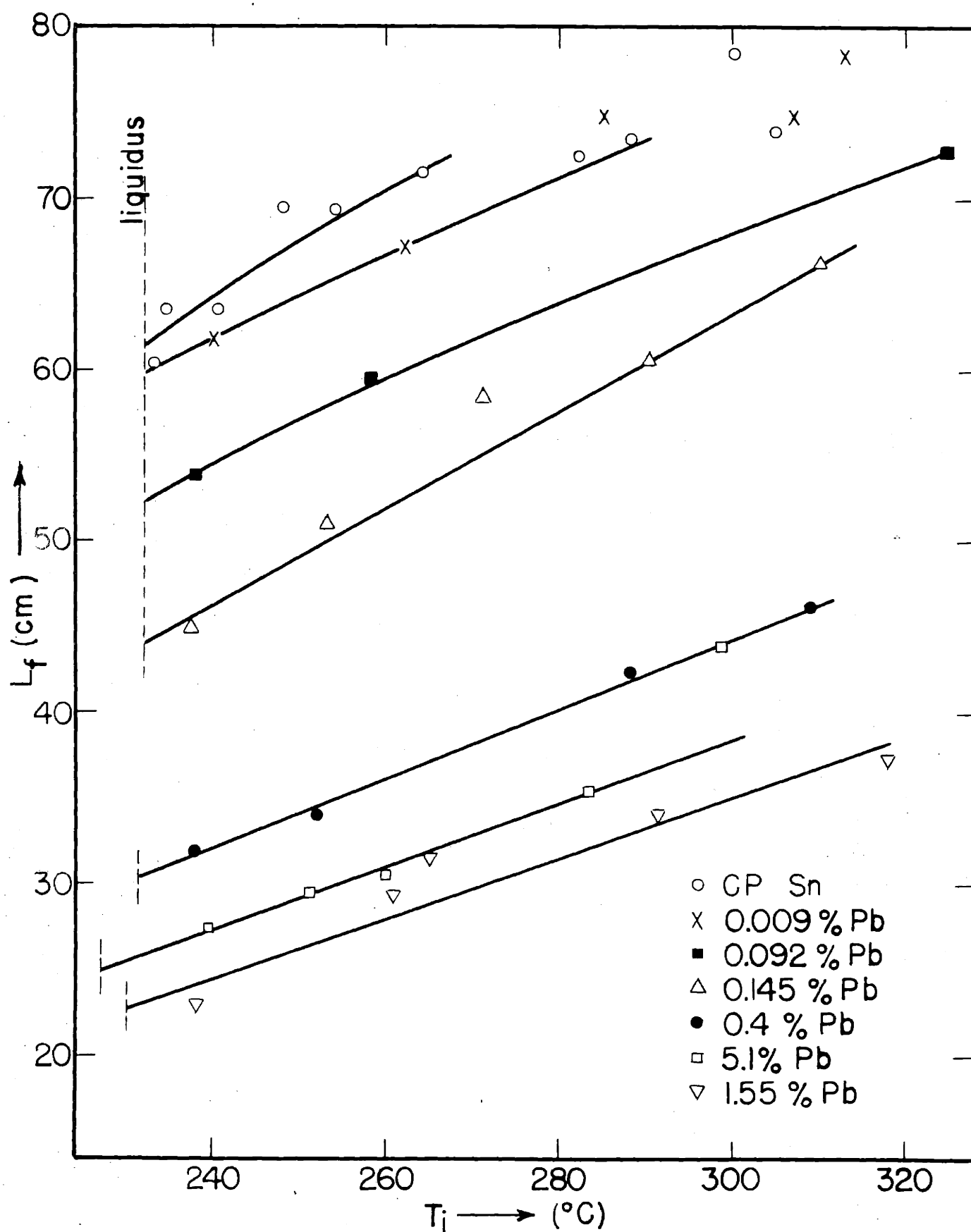


FIG. J1 FLUIDITY AT TEN INCHES METAL HEAD, SMALL TUBES

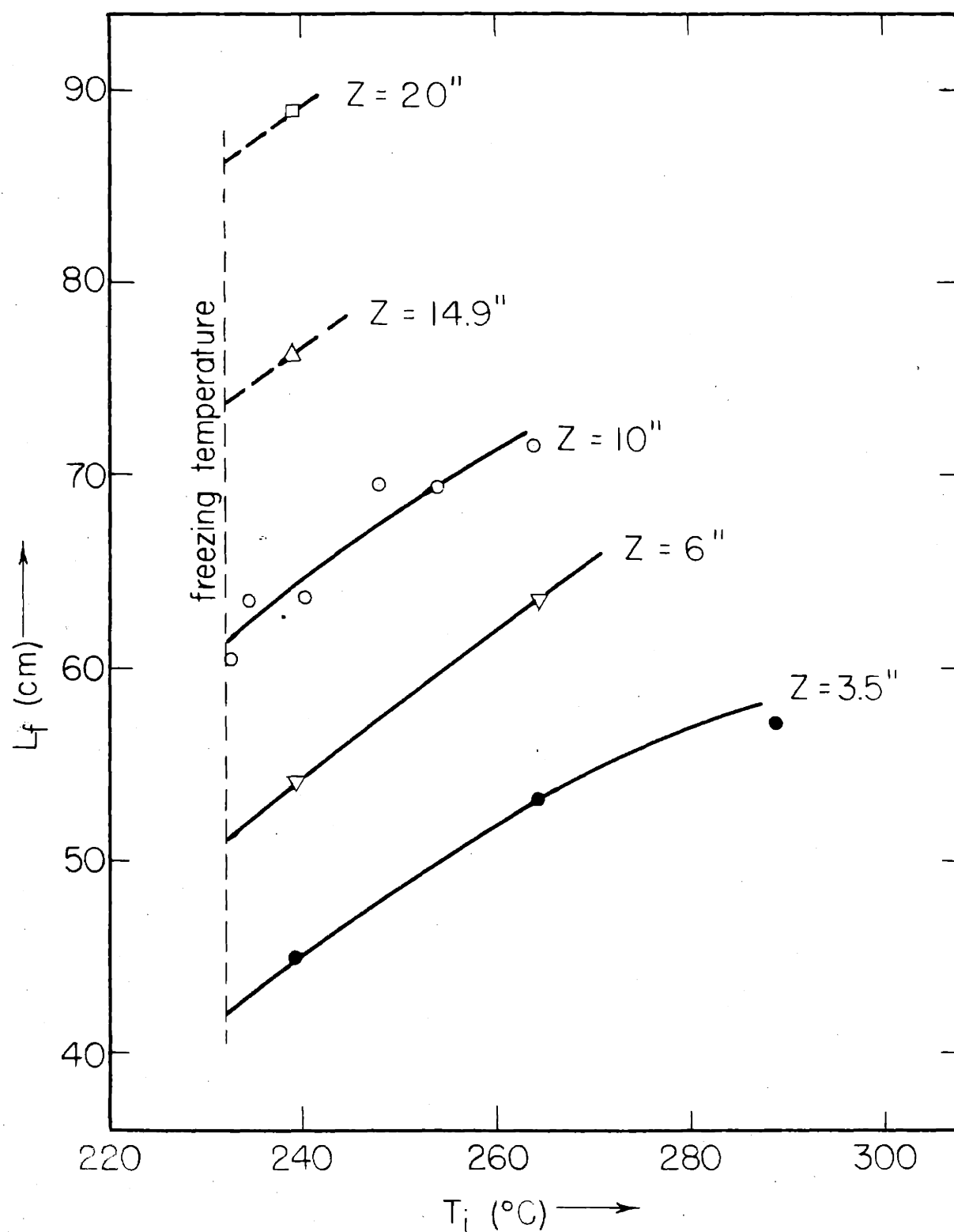


FIG. J2 FLUIDITY OF PURE TIN, SMALL TUBES

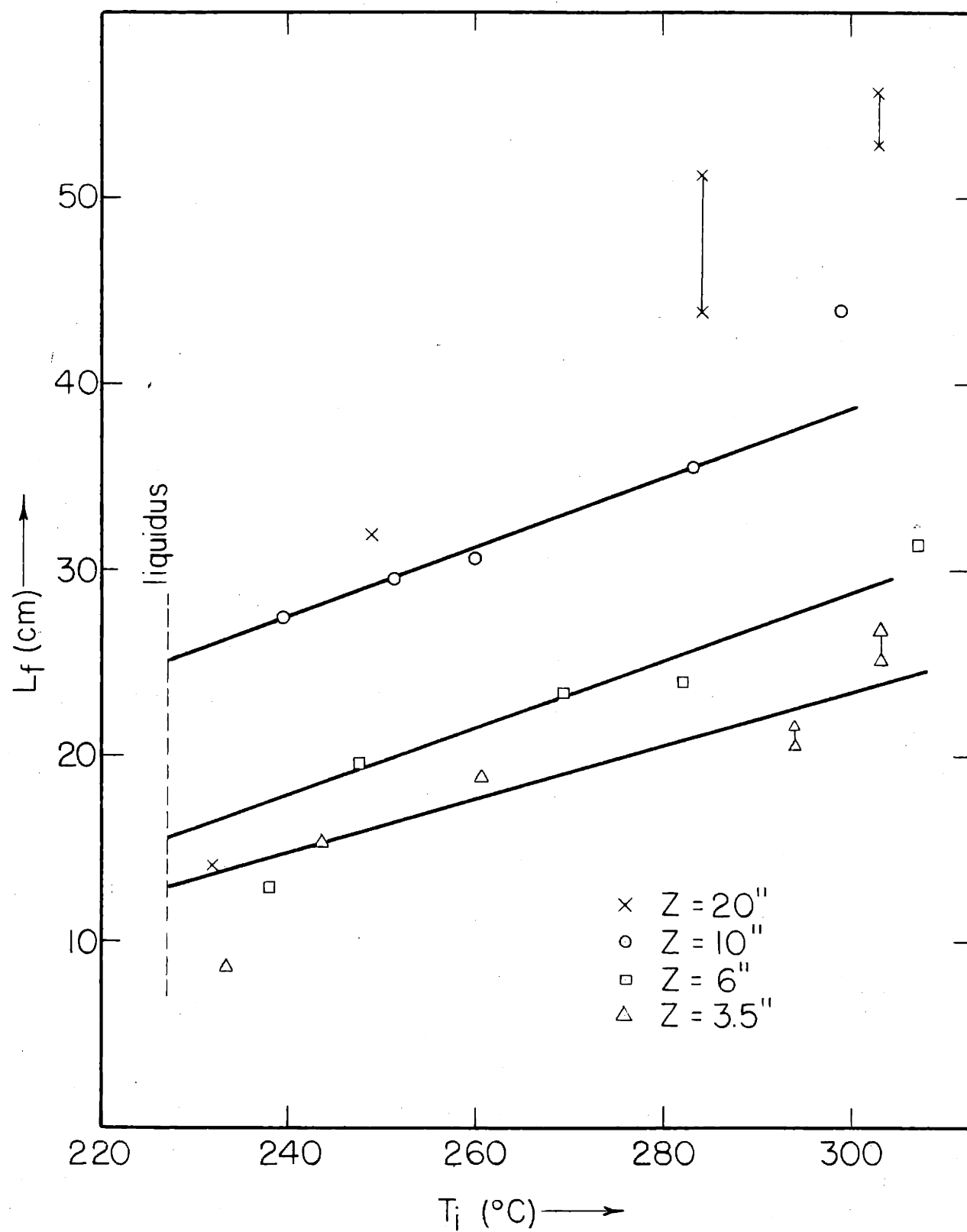


FIG. J3 FLUIDITY OF 5.1% LEAD ALLOYS - SMALL TUBES

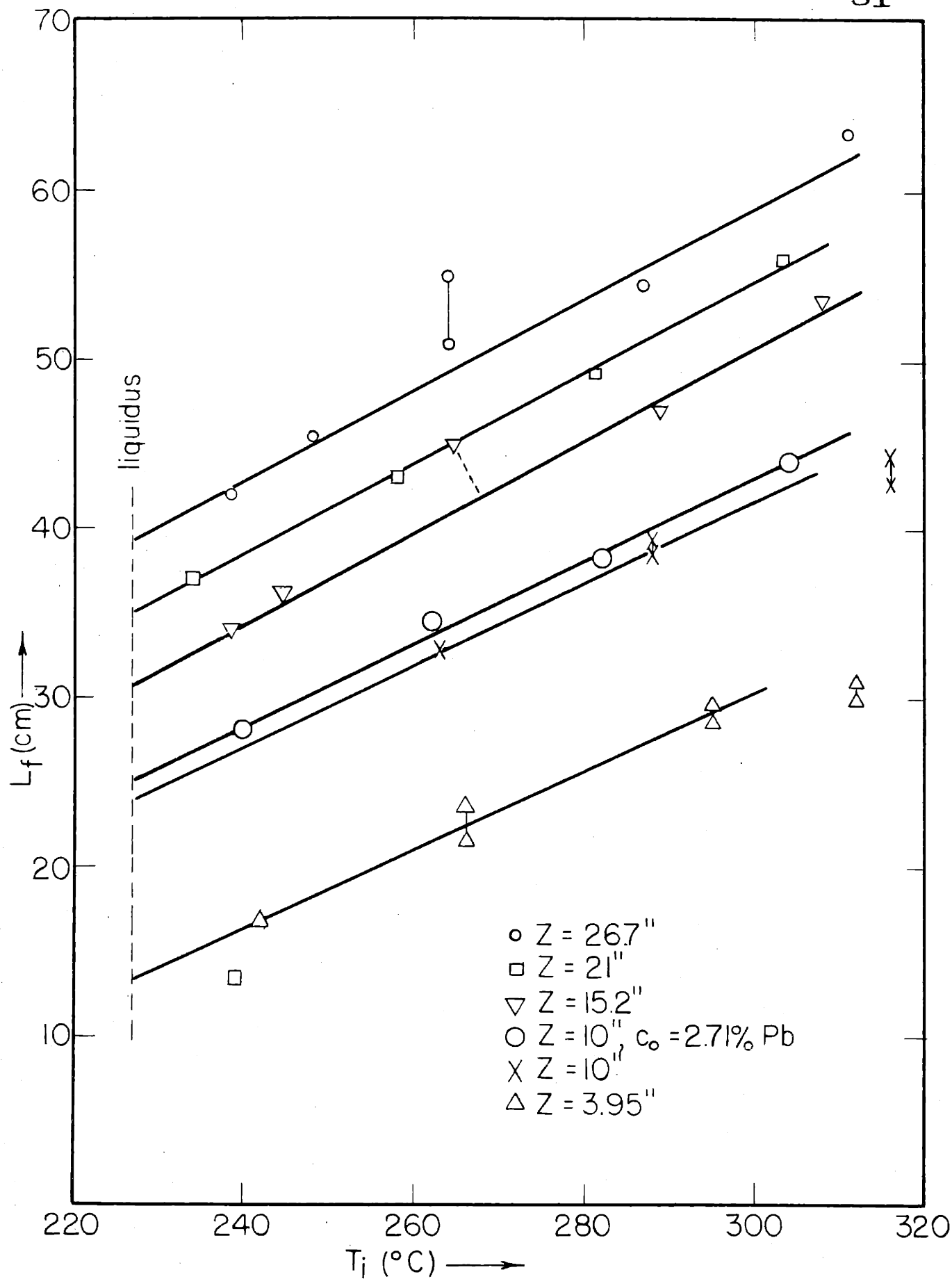


FIG. J4 FLUIDITY OF 5.1% LEAD ALLOYS - LARGE TUBES

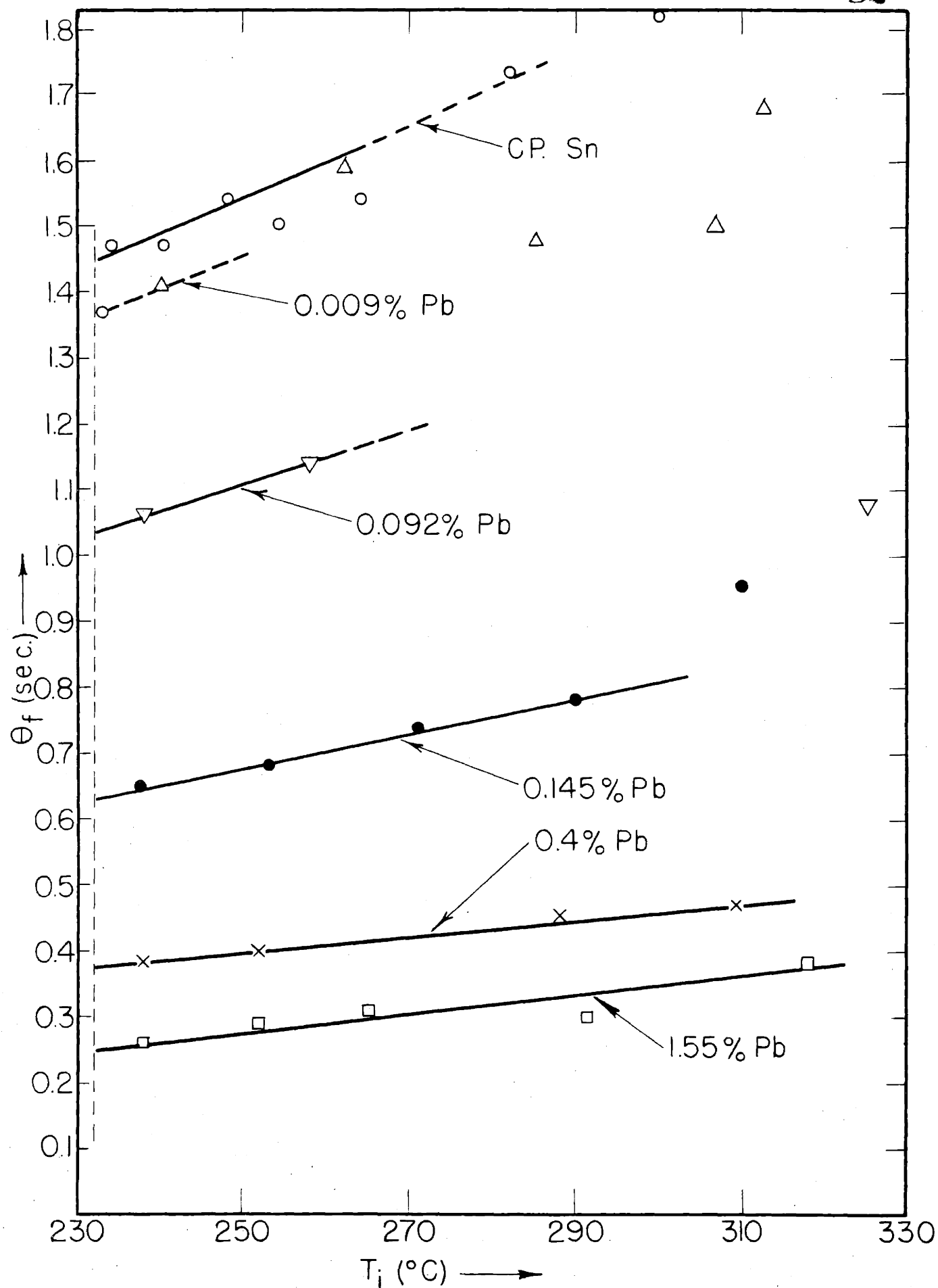


FIG. J5 FLUID LIFE AT TEN INCHES METAL HEAD

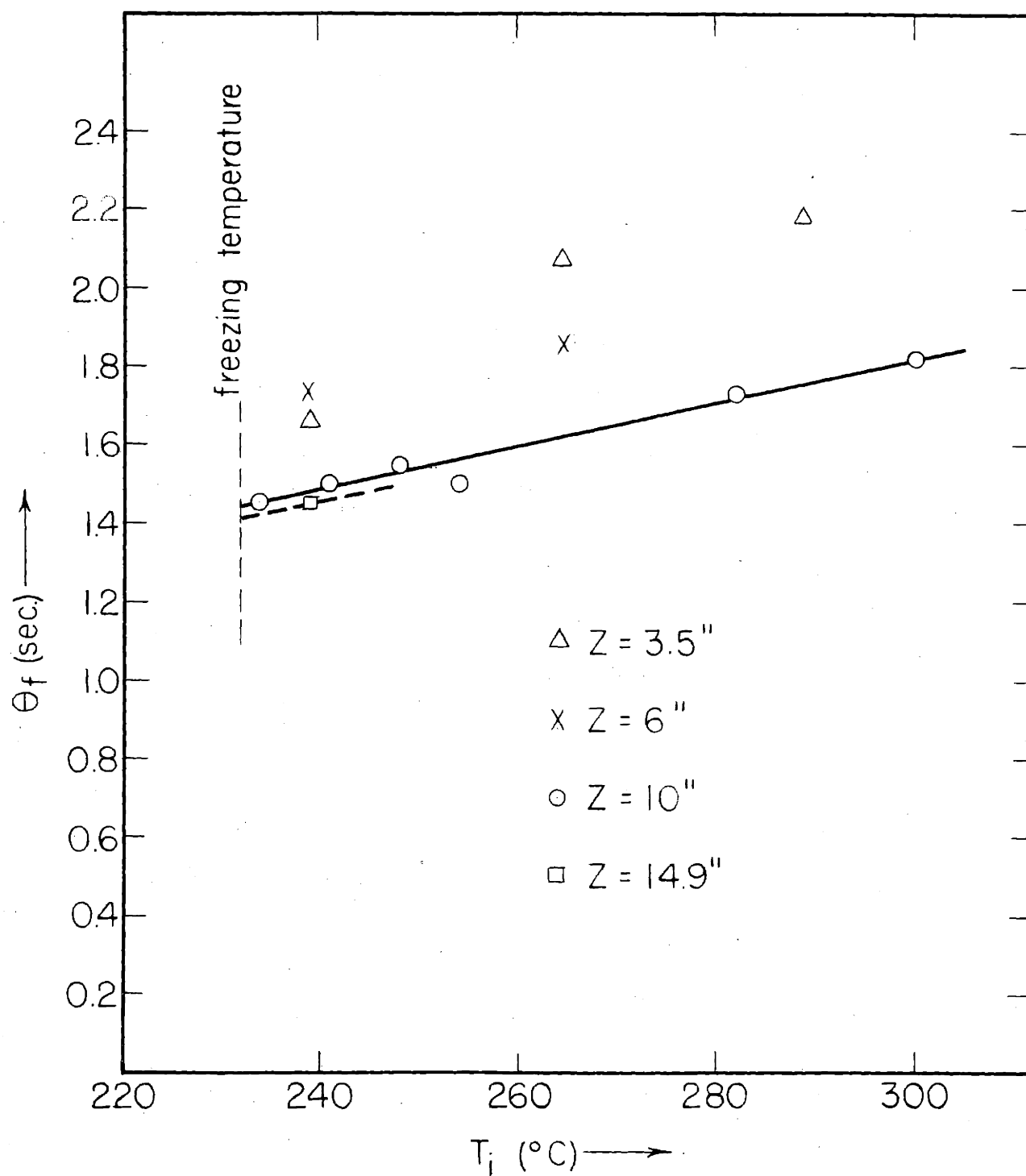


FIG. J6 FLUID LIFE OF PURE TIN, SMALL TUBES

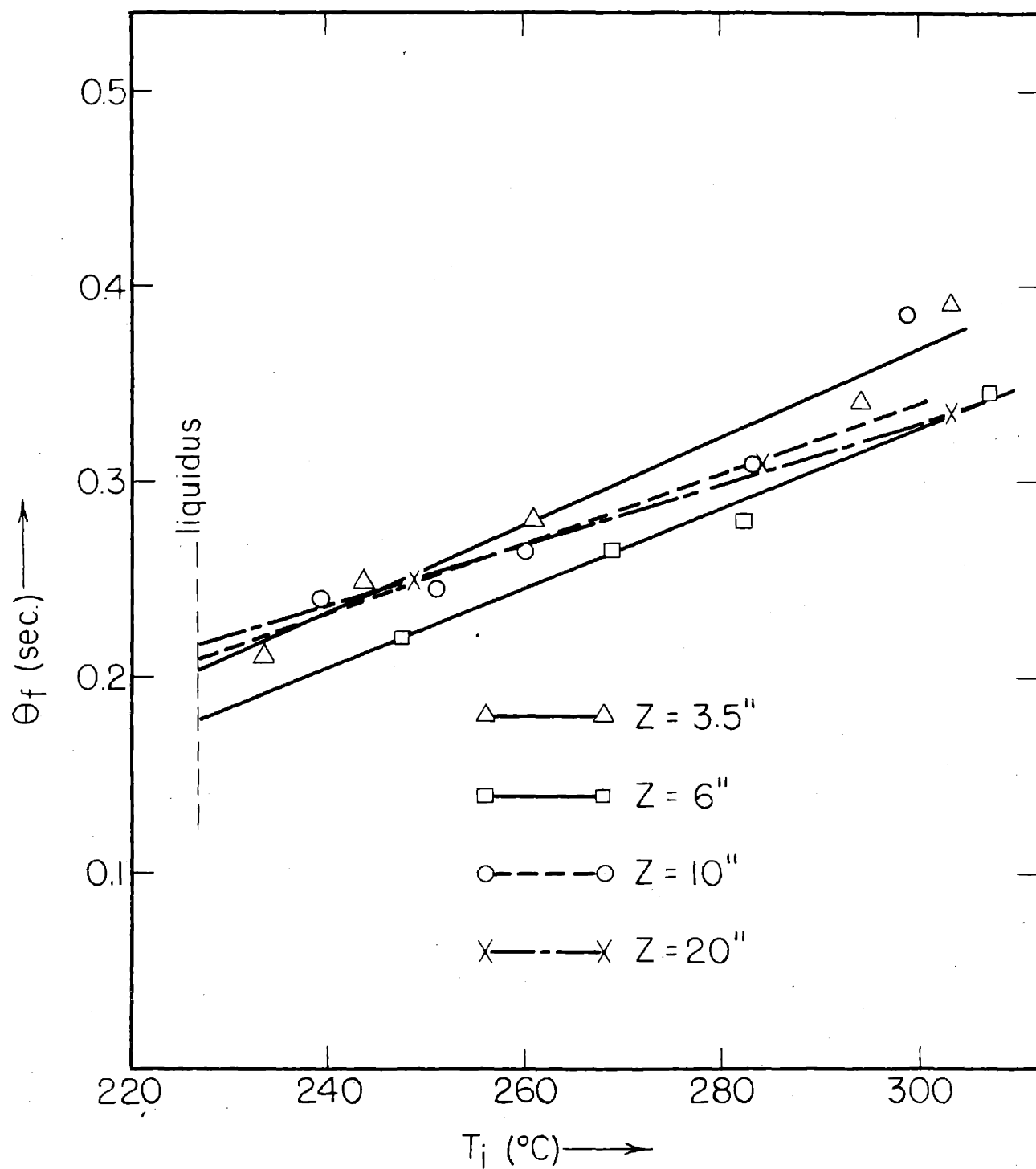


FIG. J7 FLUIDITY OF TIN-LEAD ALLOYS AS A FUNCTION OF FLUID LIFE

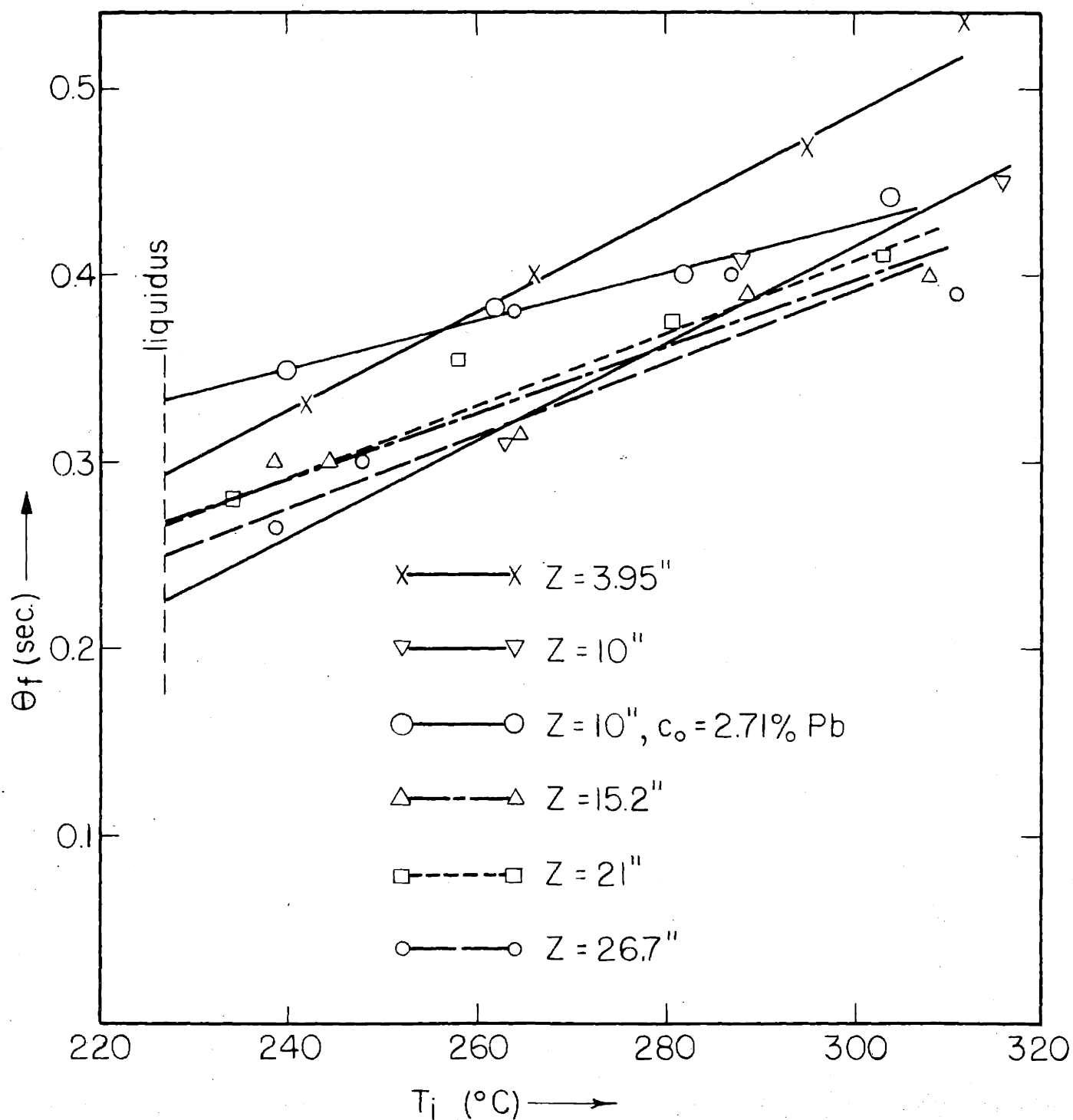


FIG. J8 FLUID LIFE OF 5.1% LEAD ALLOYS - LARGE TUBES

BIOGRAPHICAL SKETCH

The author was born in Indianapolis, Indiana on 30 November 1927. After elementary schools there and in Detroit, Michigan, he attended Broad Ripple High School in Indianapolis graduating in June 1945.

He attended Purdue University at West Lafayette, Indiana for one year before entering the U.S. Naval Academy, Annapolis, Maryland. He received a B.S. from Annapolis in June 1950.

For five years he served as a line officer in the U.S. Navy on destroyers and submarines. In August 1955 his resignation from the regular Navy was accepted and he entered M.I.T. He has been in residence at M.I.T. ever since. He received the S.M. degree in Metallurgy in September 1956.

He published an article, "Fluidity of a Series of Magnesium Alloys" in the Transactions of the American Foundrymen's Society, Volume 65, 1957.

He is a member of Tau Beta Pi and Sigma Xi honorary societies.